LUT University

From hot rock to useful energy: A global estimate of enhanced geothermal systems potential

Aghahosseini Arman, Breyer Christian

This is a Final draft version of a publication

published by Elsevier

in Applied Energy

DOI: 10.1016/j.apenergy.2020.115769

Copyright of the original publication: © Elsevier 2020

Please cite the publication as follows:

Aghahosseini, A., Breyer, C. (2020). From hot rock to useful energy: A global estimate of enhanced geothermal systems potential. Applied Energy, vol. 279. DOI: 10.1016/j.apenergy.2020.115769

This is a parallel published version of an original publication. This version can differ from the original published article.

From hot rock to useful energy: A global estimate of enhanced geothermal systems potential

Arman Aghahosseini* and Christian Breyer
LUT University, Yliopistonkatu 34, 53850 Lappeenranta, Finland
** Corresponding author - E-mail address: arman.aghahosseini@lut.fi*

Abstract

This study demonstrates the theoretical, technical, optimal economic and sustainable potential of enhanced geothermal systems (EGS) globally. A global estimate of EGS is presented in a 1˚×1˚ spatial resolution. Constructed temperature at depth maps are computed for every 1 km thick layer, from 1 to 10 km. Multiple factors such as surface heat flow, thermal conductivity, radioactive heat production, and surface temperature are involved, and obtained from various sources and assumptions. The global EGS theoretical potential is assessed. Available heat content is then estimated using technical constraints for the temperature equal to or higher than 150˚C for any 1 km depth, and presented as thermal energy and electrical power capacity. The EGS optimal economic potential is derived from the optimum depth and the corresponding minimum levelised cost of electricity. The global optimal economic potential in terms of power capacity is found to be about 6 and 108 TW_e for the cost years of 2030 and 2050, respectively. If economic and water stress constraints are excluded, the global EGS potential can be as much as 200 TW_e. Further, an industrial cost curve is developed for the levelised cost of electricity as a function of EGS technical power capacity. The findings indicate that around 4600 GW_e of EGS capacity can be built at a cost of 50 €/MWh or lower. A method is applied to measure the sustainable geothermal resource base. The obtained sustainable potential is found to be 256 GW_e in 2050. Results are presented on a country basis and globally.

Keywords: *Renewable energy; enhanced geothermal system (EGS); geothermal resource assessment; temperature at depth interval; geothermal potential; global analysis*

Nomenclature

Abbreviations

CHP	combined heat and power
CIESIN	Center for International Earth Science Information Network
EGS	enhanced (engineered) geothermal system
GEISER	Engineering Integrating Mitigation of Induced Seismicity in Reservoirs
GHG	greenhouse gas
GLiM	global lithological map
HDR	hot dry rock
IEA	International Energy Agency
IHFC	International Heat Flow Commission
MIT	Massachusetts Institute of Technology
NREL	National Renewable Energy Laboratory
ORC	Organic Rankine Cycle
SDG	Sustainable Development Goal

Symbols

A	heat production
ρ	density of the rock
C_U	Uranium content
C_{Th}	Thorium content
C_K	Potassium content
$T(z)$	subsurface temperature as a function of depth
T_0	surface temperature
q_0	surface heat flow
z	depth
k	thermal conductivity
C_p	specific heat capacity of the rock
V_c	volume of the rock
H	available heat (heat-in-place or thermal energy)
T_r	base or reference temperature
P_{theo}	theoretical potential of EGS power capacity
η_{th}	thermal efficiency
CF	capacity factor
T	mean fluid temperature
RA	technical limitations related to land availability
R_{TD}	recoverability factor of temperature drawdown

RF	recovery factor
P_{tech}	technical potential of EGS power capacity
$CAPEX$	capital expenditure
$C_{cap,well}$	geothermal well drilling and completion costs
$C_{cap,pp}$	surface plant costs
$C_{cap,stim}$	reservoir stimulation costs
$C_{cap,distr}$	fluid distribution costs
$C_{cap,expl}$	resource exploration costs
LF	learning factor
W	power plant capacity
t	year
n	number of wells
y_0	reference cost year
y_f	future cost year
$OPEX$	operational expenditure
$OPEX_{fixed}$	fixed operational expenditure
$OPEX_{var}$	variable operational expenditure
E	Electricity production
crf	capital recovery factor
FLH	full load hours
$LCOE$	levelised cost of electricity
$WACC$	weighted average cost of capital
$W_{sustain}$	sustainable power plant capacity
q_{10000}	heat flow at 10,000 m depth
SA_T	surface area at 10,000 m depth

Units

EJ	exajoules
GW	gigawatt
TWh	terawatt hour
€	euro
USD	United States Dollar

Subscripts

e	electric
th	thermal

1. Introduction

Geothermal energy as a renewable energy source is commercially available today and has great potential to contribute to the growing share of renewables to meet the global future energy demand [1–4]. Geothermal resources can supply energy throughout the year due to the constant flow of heat from the Earth. The use of geothermal energy for heat production is not new and has been practiced for thousands of years. However, for electricity generation, higher temperature resources, around 100-150˚C or higher, are needed. Thus, the availability of geothermal energy for electricity generation is limited because such high temperature resources are mostly found near volcanically active regions, abnormally high geothermal gradients, or impermeable rock around a hydrothermal system [5]. It is expected that the contribution of geothermal power to the total global electricity generation will increase due to its high potential and cost-competitiveness. Since the depletion of natural resources, such as oil and gas, and subsequent increase in price would not affect geothermal energy, it is envisaged that geothermal power gains momentum in the years to come. However, the full potential of geothermal energy has not yet been assessed on a global scale. It should be noted that although an immense quantity of heat is stored and available within the Earth , excessive production of heat resources will result in reservoir depletion or even deterioration [6].

As of 2019, thirty countries have added geothermal capacity to their total energy mix with the total cumulative installed capacity of approximately 14.6 GW globally [7]. The US continues to be the global leader, followed by Indonesia, Philippines and Turkey. In 2018, geothermal capacities were mainly installed in Turkey and Indonesia by 294 MW and 139 MW, respectively, accounting for around two-thirds of the new capacity installed collectively [8]. Turkey experienced the highest increase in geothermal power capacity, increasing from 30 MW in 2008 to 1300 MW by the end of 2018. According to the International Energy Agency (IEA) [9], global geothermal power capacity is expected to grow to more than 17 GW by 2023. Indonesia, Kenya, Philippines and Turkey are expected to have the largest capacity additions.

Geothermal heat or direct-use of geothermal energy is one of the most versatile and oldest forms of heat production. China, the US, Sweden, Turkey and Germany accounted for roughly 66% of global geothermal heat capacity installed in 2015 [10]. The major utilisation of geothermal heat is for space heating, bathing and swimming pools, which together contribute up to 80% of direct-use of geothermal energy [10]. The remaining consumption of geothermal heat is for domestic hot

water, agriculture (greenhouse heating, agricultural pond heating and agricultural drying), industrial process heat, cooling and snow melting applications [11]. Geothermal (ground-source) heat pumps are one of the fast growing applications for direct-use of geothermal energy, which allow for reduction in fossil fuel consumption and GHG emissions, as well as economic benefits [12,13]. The heat can be collected from different depths depending on the geothermal heat system. Horizontal ground heat exchangers extract the heat at depths of 1 to 2 meters. Ground water wells work at depths of 4 to less than 50 meters. Energy pipes collect heat at depths of 5 to 45 meters, and heat collection for borehole heat exchangers is between 10 to 250 meter depths [14]. As of 2015, the leading countries in terms of heat pumps installed capacity are the US, China, Sweden, Germany and France, with a total installed capacity of 38.8 GW_{th} [10].

There are two types of geothermal energy systems: conventional geothermal systems (hydrothermal) and enhanced (engineered) geothermal systems. The latter was previously known as Hot Dry Rock (HDR) and will be referred to as EGS hereafter in this paper. The majority of recently built and under construction hydrothermal and EGS geothermal power plants use binary-cycle technology [8]. The advantage of binary-cycle technology to other ordinary geothermal technologies is the operation with relatively low-temperature resources. However, existing geothermal plants use flash-steam and dry-steam technologies mostly, which are suitable for high-temperature resources. As mentioned earlier, conventional geothermal systems are restricted to specific geographical locations. In addition, permeable aquifers are the basis for hot water production in the standard hydrothermal technologies. In contrast, EGS can be built in larger areas, in different parts of the world, by creating a subsurface fracture system in the hot rock through hydraulic stimulation. Further, since the heat is extracted from hot basement rock at greater depths, there would be less natural permeability and fluid content. In the EGS process, high-pressure cold water travels through fractions in the rock via injection wells to capture heat from rock at great depths and returns to the surface via production wells as hot water. Then, the heat of hot water is converted into electricity using a steam turbine or a binary power plant. The cooled down water is re-injected into the ground to heat up again in a closed loop. EGS emits a very small to zero amount of GHG emissions [15]. Having said that, the average GHG emissions associated with geothermal power plants is around 120 gCO_2/kWh_e, which is relatively lower than that of fossil fuels power plants [16]. It is expected that the technology improvements, such as re-injection, will decrease the amount of GHG emissions significantly to 10 gCO_2/kWh_e [16]. EGS is comparable with other

renewable energy technologies with regards to GHG emissions and environmental impacts, and in some cases have lower environmental impacts [17]. The GHG emissions from EGS range from 3.8 to 45.6 gCO_2-eq/kWh_e, depending on the selected applications [17].

The EGS potential estimation for the US has been proposed and evaluated by Tester et al. [18], Blackwell et al. [19], Augustine [20] and Lopez et al. [21]. Tester et al. [18] assessed the feasibility of providing 100 GW_e electric capacity of EGS by 2050. They concluded that the EGS potential is even larger in the long-term, and achieving such a target is viable. Blackwell et al. [19] analysed the EGS potential for the conterminous US using temperature at depth (3-10 km) maps. It is reported that if only 2% of the EGS resource is developed, the produced energy would be 2500 times the annual primary energy consumption in the US in 2006. Augustine [20] presented the potential electric capacity of the US geothermal resources and the respective costs. The total identified hydrothermal and EGS capacities are about 36.4 GW_e and 15,915 GW_e, respectively. Additionally, the optimum reservoir depth has been determined using the minimum levelised cost of electricity (LCOE) at each data point. Lopez et al. [21] explored the technical potential for EGS using temperature at depth data. Similar to Augustine, the quantitative analysis method has been applied in order to find the optimum depth at the minimum LCOE. The US total technical potential for hydrothermal geothermal systems and EGS is evaluated to be around 38 GW_e and 4000 GW_e, respectively.

A geothermal resource estimation was carried out for Korea [22] based on constructed temperature at depth maps. The calculated subsurface geothermal energy ranges between 16.7 ZJ ($4.6 \cdot 10^5$ TWh_{th}) at 1 km depth and 101 ZJ ($280 \cdot 10^5$ TWh_{th}) at 5 km depth. Chamorro et al. have conducted studies for EGS potential estimation in Europe [23] and Iberian Peninsula [24]. Similar methods have been applied in both studies. The technical potential in terms of electrical power capacity is identified to be around 700 GW_e in the Iberian Peninsula and more than 6500 GW_e in Europe. Moreover, for the case of Europe, a sustainable potential term has been defined where not all the available heat content in the basement rocks can be extracted. Applying this constraint affected the technical potential estimation drastically and the final sustainable potential is found to be 35 GW_e. The potential for geothermal energy in Germany has been evaluated [25]. Under the most optimistic assumptions, the available land area for constructing EGS plants is identified to be 89,000 km^2, which can consist of 13,450 EGS plants with a maximum electric capacity of 474 GW_e. An EGS analysis based on the subsurface temperatures data and minimum LCOE has been

conducted in Europe [26]. The potential is deduced to be 19 GW_e in 2020, 22 GW_e in 2030 and 522 GW_e in 2050. The temperature at depth calculations have also been performed to estimate the EGS potential in Great Britain [27]. The results indicate that the total technical potential is about 222.4 GW_e for the depth of 6.5 km and temperature greater than 150˚C. An optimal design of EGS has been assessed for the case of Switzerland considering environmental impacts [28]. The findings reveal that the shallower depths, 3500-6000 m, are more favourable for a district heating network while deeper depths are suitable for electricity production. However, the choice of appropriate technologies and applications might vary depending on the considered criteria. Hofmann et al. [29] studied the potential for EGS in the province of Alberta in Canada and concluded that Cooking Lake formation and Basal Sandstone are the most promising reservoirs, among the investigated formations, for heat extraction, even though the associated costs are higher than shallower formations. It has been claimed that China [30] has abundant EGS resources, especially in Southern parts of the country such as Yunnan, Tibet, and Southeast Coast. The evaluated EGS potential in China is about $7 \cdot 10^9$ TWh_{th} [31]. The Chinese Academy of Geological Sciences stated that the technical extractable geothermal resources with temperature of higher than 150˚C is around 8500 MW_e [32]. Xia and Zhang [32] concluded that despite the availability of geothermal resources, several internal and external factors influence the development of geothermal energy in China as well as in other countries globally. These include, but not limited to, insufficient exploration of resources, lack of access to the necessary data for detailed analysis, shortage of sufficient policy support, intense competition with other energy resources, and mismatch between supply and demand.

A Protocol for estimating the EGS potential has been proposed [33]. The Protocol set a framework, for both theoretical and technical geothermal potential estimation in different regions, using consistent methodologies and assumptions. The main goal of the Protocol is to make the results of different regions comparable for better understanding of EGS potential across the world. The current research work follows the Protocol recommendations for EGS estimation globally, where applicable, and also delved into other sources, methods and assumptions. This study is structured as follows: in section 2, the materials and methods used to evaluate the EGS potential globally are explained; in section 3, the results of modelling are presented; in section 4, a comprehensive discussion regarding the EGS potential assessment in this study, comparison of the results with

other studies, and limitations and uncertainties are carried out; in section 5, a summary of the presented and discussed results is given.

2. Materials and methods

In this study, the world is clustered into a regular gridding interval of 1 degree by 1 degree, 1˚×1˚, to evaluate the EGS potential. This assumption is different with the 5'×5' interval (5' = 5 minutes = 0.0833˚) proposed by Beardsmore et al. [33] in the Protocol, due to limited access to the data on a global level. It is challenging to find reliable and accurate data in such high spatial resolution on a large-scale. In case the data were available for the gridded cells, the actual data are collected and administered. If the data does not exist or is not accessible, some assumptions were made to provide the data in the desired format. For estimating the EGS potential, various input data are required, which are described and investigated in the following sub-section. The modelling is carried out mainly using QGIS software [34] for geospatial data analysis and Matlab software [35] for programming and simulation. Once the input data are gathered, the temperature at depth maps are constructed. Then, the available heat for each depth interval in each gridded cell are computed. Next, the EGS theoretical and technical potentials are estimated. Finally, the optimum depth is identified and the respective optimal potential based on the given data is obtained. The optimum depth is determined by finding the first cell at each depth interval with temperature ≥150˚C. Ultimately, there is a minimum LCOE at which all the EGS components are at their optimal points. The simplified framework for the EGS potential estimation is presented in Figure 1. It is crucial to point out that although the authors strive to gather data that is as accurate as possible, there is always room for improvement. Thus, the basic structure introduced and modelled in this study can be disseminated to improve the input data, modify the methods, and change the applied assumptions and constraints, especially for country and small-scale studies. This will pave the path for future EGS potential estimation for different case studies and provide more detailed insights for policy-makers and project developers to enhance the utilisation of renewable energy across the world.

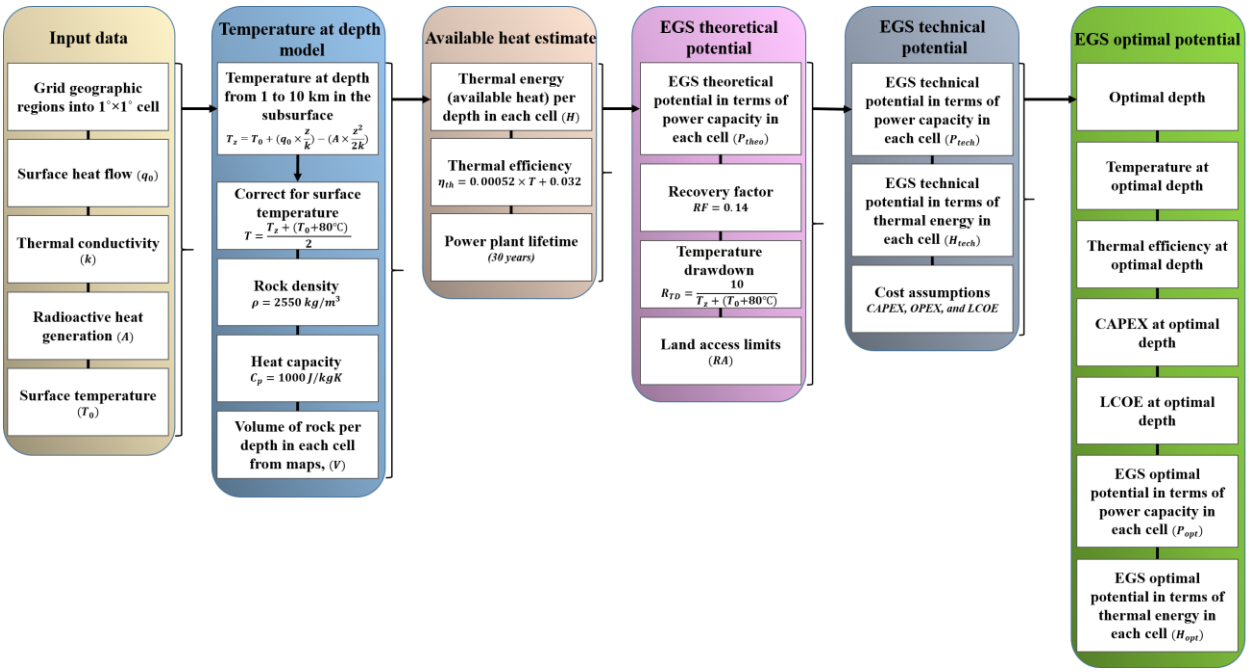

Fig. 1. Flowchart for EGS potential estimates including the main inputs and outputs of the model.

2.1 Heat flow

The primary step to estimate the EGS potential is to model temperature at depth. Several data components are required to obtain the temperature of each 1 km thick layer beneath the surface, i.e. the depths between 1 km and 10 km. As a starting point, a heat flow map should be drawn. The surface heat flow data is collected from various resources. The majority of heat flow data comes from the International Heat Flow Commission (IHFC) database [36], American Association of Petroleum Geologists [37], and Pollack et al. [38]. Further, the heat flow data in Europe [39,40], Arctic [41], Mid-Atlantic Ridge [42], Turkey [43], Brazil [44], Cameroon [45], Nigeria [46], Eastern Africa and the North Sea [47], Iran [48], the Republic of Korea [49], Southeast Asia [50], Mexico [51,52], South America [53], and some other countries or regions [54] are collected and compared with the IHFC database. Then, the data is calibrated and combined with the database. In addition, borehole data are used for verification and completion of the datasets, which is gathered from National Centers for Environmental Information [55]. Based on the given databases, the required data from borehole sites have been extracted, such as ground surface temperature (T_0), temperatures at the given depths below the surface, mean conductivity, mean thermal gradient and the locations of the boreholes. Clusters of data points within each grid cell are averaged. It is clear

that the more detailed input data is found, the higher accuracy of the results can be expected. Nevertheless, the global coverage of heat flow measurements is falling short in many areas. To cover all the cells with the respective input values, the existing data can be extrapolated. For a better estimation, it is crucial to select the best possible proxies. Therefore, a method introduced by Goutobe et al. [56] is adopted to fulfil the missing data points. Several geological and geophysical datasets, such as mantle seismic velocity, physical and tectonic features in the crust and geodynamic setting, have been applied to better capture the current situation of global surface heat flow. The "Best combination method" and "Similarity method" are the two appraised methods to determine the missing heat flow data. The Similarity method is found to be a better approximation for medium- to large-scale trends, even though the model lacks in validation of short-scale features of heat flow. The cross-validation carried out for both approaches presented better accuracy for the Similarity method [56]. In the Similarity method, if a sample has some degree of similarities with the target function, that sample receives a certain weight. The degree of similarities is defined as the number of similar terrestrial components between the target and the sample and obtained via an exponential function. This method is described at length in [56], and employed in the current study. When the raw heat flow measurements exist, the actual data points are utilised. Otherwise, the data produced from the similarity method [56] is employed. It should be noted that Davies [57] also analysed the global surface heat flow data on a 2˚×2˚ grid cell size using the age of the oceanic crust, the raw heat flow data measurements and the correlation between heat flow and geology. The 2˚ scale is selected to have more coverage of the raw data. The current global surface heat flow map has some level of similarity to that presented by Davies [57]. Both articles pursued the average heat flow measurements, where available, and applied proxies to estimate the heat flow for areas with no data available. There are some advantages and drawbacks in both studies, but they roughly present the global heat flow data, which is a fundamental database for many fields of research. Global surface heat flow data is shown in Figure 2a.

2.2 Thermal conductivity

Most of the heat flow data is linked to supplementary information such as thermal conductivity and temperature gradients that can be used to acquire temperature at various depths beneath the

Earth's surface. The datasets might include negative and none specified values, which have been corrected while preparing the final database. Thermal conductivity data with odd values are excluded from the database. Similar to heat flow, the measured thermal conductivity data is not sufficient to cover the entire global surface. Therefore, the correlation between geology and thermal conductivity are assumed to be the best proxy to clarify the thermal conductivity for the missing areas. To do so, a high resolution global lithological map (GLiM) [58] is employed, as shown in Figure 2b. Among a wide range of thermal conductivity values for different rocks [33,59–62], a mean value is taken for each lithological formations. The list of lithological formations, typical rock types and their respective thermal conductivity values is tabulated in Table 1. The thermal conductivity map is illustrated in Figure 2c. For the areas with no data availability, a value of thermal conductivity of 2.5 W/mK was assumed, as a global mean in situ thermal conductivity [33,61].

Table 1. List of lithological classification, typical rocks samples in each class and the mean thermal conductivity allocated to each class [33,59–62]

Lithological class	**Examples**	**Thermal conductivity (W/mK)**
Unconsolidated sediments	Dune sands, alluvial deposits, loess, swamps	1.9
Siliciclastic sedimentary rocks	Sandstone, mudstone, greywacke	3.4
Pyroclastics	Tuff, volcanic breccias, ash	1.4
Mixed sedimentary rocks	Interlayered sandstone and limestone, shaley marl	3.3
Carbonate sedimentary rocks	Limestone, dolomite, marl	3.7
Evaporites	Gypsum, anhydrite, halite, salt pan	5.4
Acid volcanic rocks	Rhyolites, trachytes, dacites	1.4
Intermediate volcanic rocks	Andesites	1.8
Basic volcanic rocks	Basalts (tephrites, tholeites, and lamprophyres)	1.8
Acid plutonic rocks	Quartz, granites, quartz-diorites, quartz-monzonites	2.5
Intermediate plutonic rocks	Diorite, monzonite, syenite	2.1
Basic plutonic rocks	Mafic minerals, like gabbro and peridotite, ultrabasic species like norite, ophiolite	2.9
Metamorphic rocks	Shales, gneiss, amphibolite, quartzite	3.5
Water Bodies	Lakes, rivers, coastal oceans	0.6
Ice and Glaciers	Ice	2.2
No Data	Undefined	2.5

2.3 Radiogenic heat production

The heat generation value of the upper crustal rocks is typically obtained from three radioactive elements, Uranium, Thorium and Potassium, as shown in the Equation 1 [63].

$$A = 10^{-5}\rho(9.52C_U + 2.56C_{Th} + 3.48C_K) \quad (1)$$

where A is heat production (μW m^{-3}), ρ is the rock density (kg m^{-3}), C_U is the Uranium content (ppm), C_{Th} is the Thorium content (ppm) and C_K is the Potassium content (ppm). The units for all heat production constants are in W kg^{-1}.

However, the measured radioactive components are limited to specific areas. Goutorbe et al. [56] made two assumptions to achieve a representative global heat production on 1˚×1˚ grid size. First, the median value of available heat production in each grid cell is taken. Second, the mean heat production is extrapolated over homogenous continental provinces. The latter approach is considered in this study, but rather than extrapolation over provinces, the extrapolation is conducted by countries, as presented in Figure 2d.

2.4 Surface temperature

Global surface temperature data for the year 2005 is taken from NASA database [64]. The datasets are available for the periods 1984-2005. However, the year 2005 is selected since it is the most recent data available [65]. In addition, NASA provides gridded data, which makes it suitable for the current study. The map of global surface temperature is given in Figure 2e.

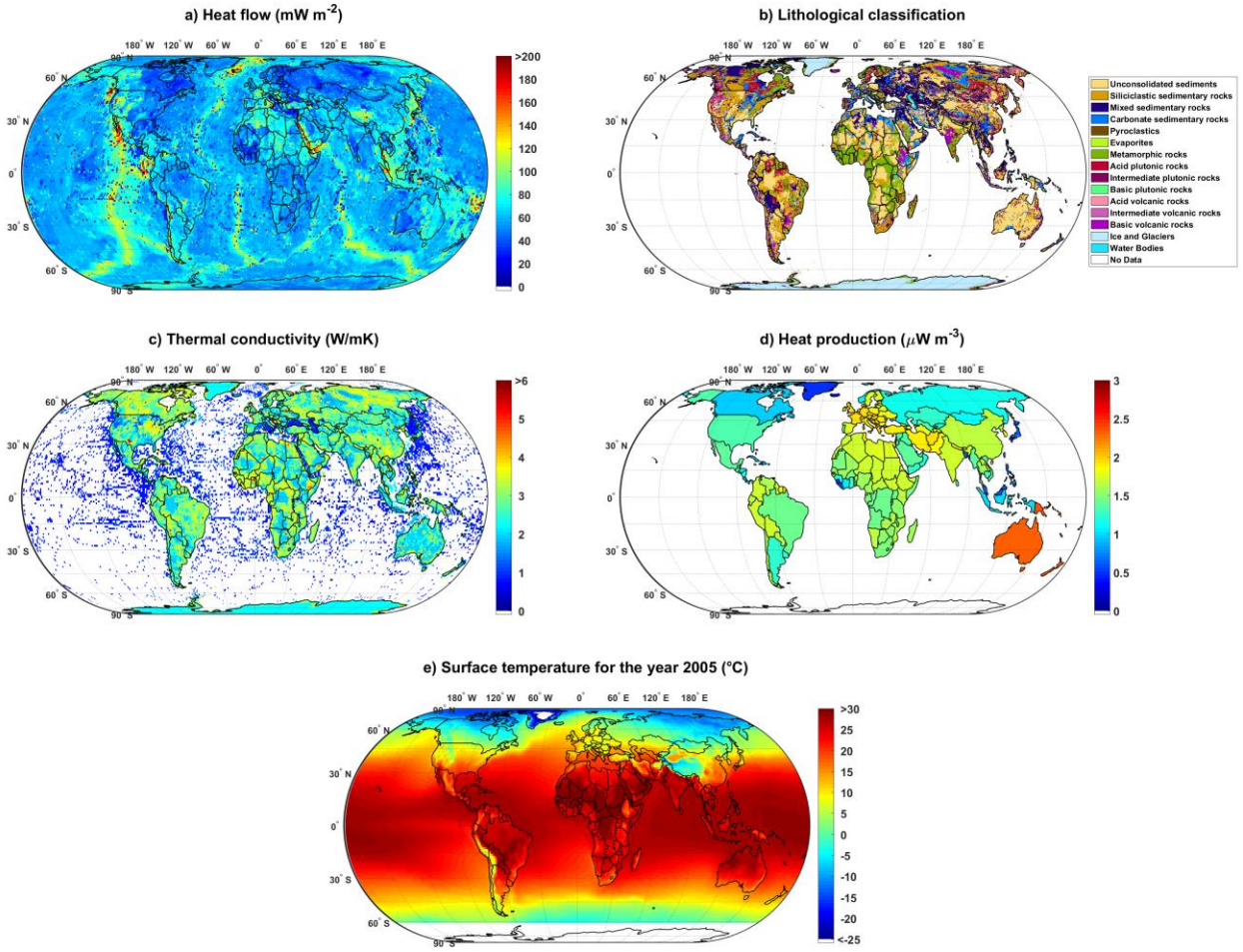

Fig. 2. Global overview of the input data for the EGS model; a) global surface heat flow, including both actual measured data points and adopted Similarity method for extrapolation; b) global lithological formations, modified after Hartmann and Moosdorf [58]; c) global thermal conductivity, including both actual measured data points and the correlation between geology and thermal conductivity; d) global radiogenic heat production; e) global surface temperature for the year 2005. The white colour in the colourbar indicates that no data is available.

3. Results

3.1 Temperature at depth

To derive temperature as a function of depth, a steady state is assumed without heat advection processes such as magmatism occurrence, intense erosion and hydrothermal convection [5]. All the above mentioned phenomena can occur only in short period of time when equilibrium thermal regime of the continental crust is considered. Therefore, the simplest form of Fourier law can be

calculated based on the Equation 2. In this condition, a constant thermal conductivity, a depth-dependent temperature field, and suitable boundary conditions for continental crust are expected.

$$T(z) = T_0 + (q_0 \cdot \frac{z}{k}) - (A \cdot \frac{z^2}{2k}) \quad (2)$$

where *T(z)* is the subsurface temperature as a function of depth, T_0 is the surface temperature, q_0 is the surface heat flow, *z* is the depth, *k* is the thermal conductivity, and *A* is the heat production.

Once the temperature at depth *z* is computed in the subsurface down to 10,000 m, a mean estimated temperature profile is available for each 1˚×1˚ grid cell. As a result, the temperature maps for specific depth slices can be constructed, as shown in Figure 3.

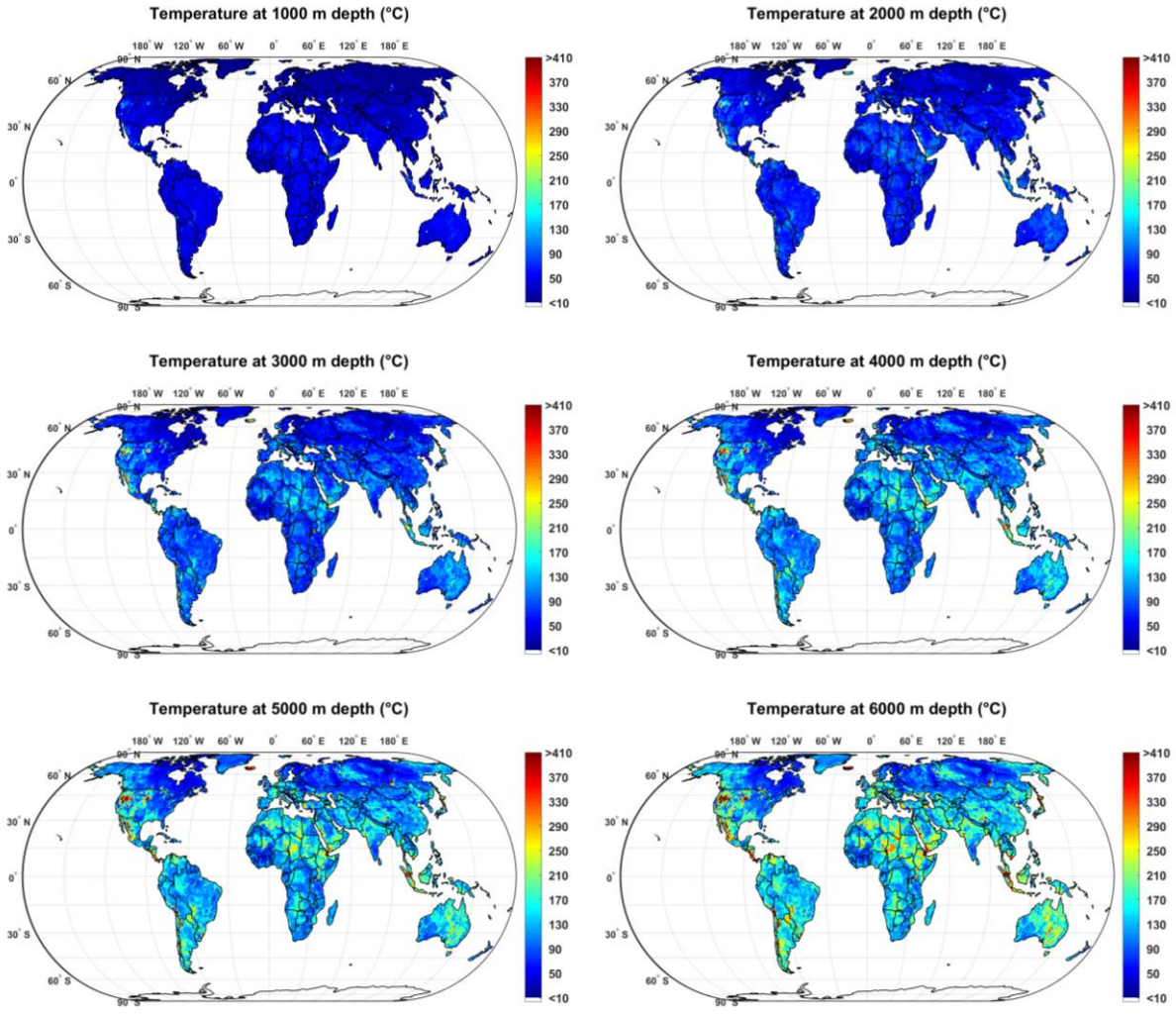

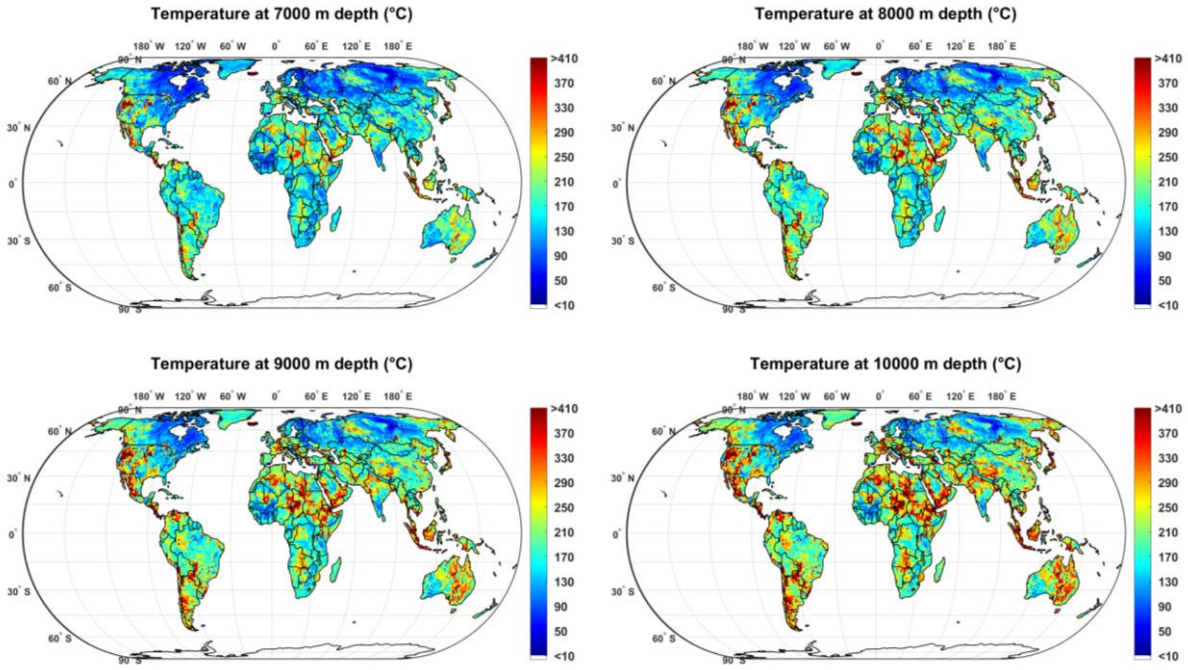

Fig. 3. The global maps of estimated temperature at various depths, from 1000 m to 10,000 m, beneath the Earth's surface.

3.2 Theoretical potential of EGS

To estimate the theoretical potential of EGS, the available heat stored underground within a volume of rock has to be calculated. The heat content within a rock is commensurate with temperature at every depth interval, specific heat capacity, density and volume of the rock. It is assumed that the density (ρ) and specific heat capacity (C_p) of the rock are constant and equal to 2550 kg/m^3 and 1000 J/kg K, respectively. In order to calculate the volume (V_c) of each 1˚×1˚ grid cell at 1000 m depth interval, the surface area of each cell is primarily individually calculated. It should be noted that the surface area of each 1˚×1˚ grid cell varies depending on latitude. The areaint function in Matlab [35] is used for determining the area of each cell. This function is a numerical computation, using a line integral based on Green's Theorem. Once the surface area of each cell is derived, the volume of a 1000 m thick interval of crust can be calculated. Finally, the available heat for each depth interval in each cell is identified using Equation 3. Since each depth contains a different amount of thermal energy, the available heat is calculated in a 1000 m thick volume of crust.

$$H = \rho \cdot C_p \cdot V_c \cdot (T_z - T_r) \cdot 10^{-18} \quad (3)$$

where H is the total available heat (exajoules, EJ), ρ is the density of rock, C_p is the specific heat capacity of rock, V_c is the volume of rock, T_z is the temperature at depth interval calculated in section 3.1, and T_r is the base or reference temperature. In the research conducted by Tester et al. [18] and Blackwell et al. [19], the base temperature is considered to be the same as the mean ambient air temperature. However, this investigation assumed a base temperature of 80˚C above mean annual surface temperature at each location, as suggested by Williams et al. [66] and the guidelines of the Protocol [33]. The assumption is made based on the measured temperature to which the crust can be theoretically cooled down. William et al. [66] assumed a base temperature of 75°C (Chena Hot Springs) in Alaska and 90°C (Amedee, California) in the 48 states of the US. A mean temperature of 80˚C above mean annual surface temperature is later proposed by the Protocol [33], and adopted by [26] and [27]. Therefore, the base temperature is calculated based on Equation 4. T_0 is the surface temperature at each grid cell.

$$T_r = T_0 + 80℃ \quad (4)$$

Table 2 shows the heat content values for V_c centred at depth for 1 km slices using the discussed assumptions and equations above. The values of heat content are classified by 50˚C intervals starting from 150˚C to 400˚C and above. The first number in each temperature range is set to equal to or higher than the given temperature and the last number set to less than the given number in that range. These values represent the stored thermal energy underground and not the amount of electrical power that can be generated. A histogram of available heat content as a function of depth is provided in Figure 4. As can be seen, a significant geothermal resource base occurs between the depths of 6 and 10 km, and to some extent at the depths of 3 and 4 km, in the temperature range of 150 to 300˚C. It is clear that as the drilling process goes deeper, a higher temperature and therefore more heat content is expected. However, at higher depths, the distribution of temperature might change. Consequently, the availability of thermal energy varies in different temperature ranges. For instance, the heat content at the depth of 10 km for the temperature range of 150-200˚C is slightly lower than that at the depth of 8 km. At higher depths there is less heat content for the lower temperature range, but more heat content at higher temperature range. Maps of the estimated theoretical heat potential at various depths are illustrated in the Supplementary Material (Figure S4).

Table 2. Heat-in-place or available heat content (stored thermal energy) for the global EGS theoretical potential estimates for 1 km depth intervals.

Heat content (TWh_{th})	150-200°C	200-250°C	250-300°C	300-350°C	350-400°C	≥400°C
1 km	2.8E+07	7.8E+06	3.6E+06	4.3E+06	0.0E+00	3.7E+06
2 km	2.5E+08	8.2E+07	2.7E+07	2.3E+07	1.5E+07	3.0E+07
3 km	1.0E+09	2.2E+08	2.0E+08	5.8E+07	3.3E+07	1.0E+08
4 km	3.4E+09	7.6E+08	2.3E+08	1.7E+08	1.7E+08	2.2E+08
5 km	6.1E+09	2.2E+09	6.4E+08	2.4E+08	1.5E+08	5.7E+08
6 km	8.0E+09	4.0E+09	1.5E+09	5.8E+08	2.4E+08	8.8E+08
7 km	9.0E+09	5.7E+09	2.7E+09	1.2E+09	5.5E+08	1.3E+09
8 km	9.7E+09	6.9E+09	4.1E+09	2.0E+09	9.3E+08	1.9E+09
9 km	9.5E+09	7.5E+09	5.2E+09	3.0E+09	1.6E+09	2.7E+09
10 km	8.6E+09	8.0E+09	6.1E+09	4.1E+09	2.2E+09	4.0E+09

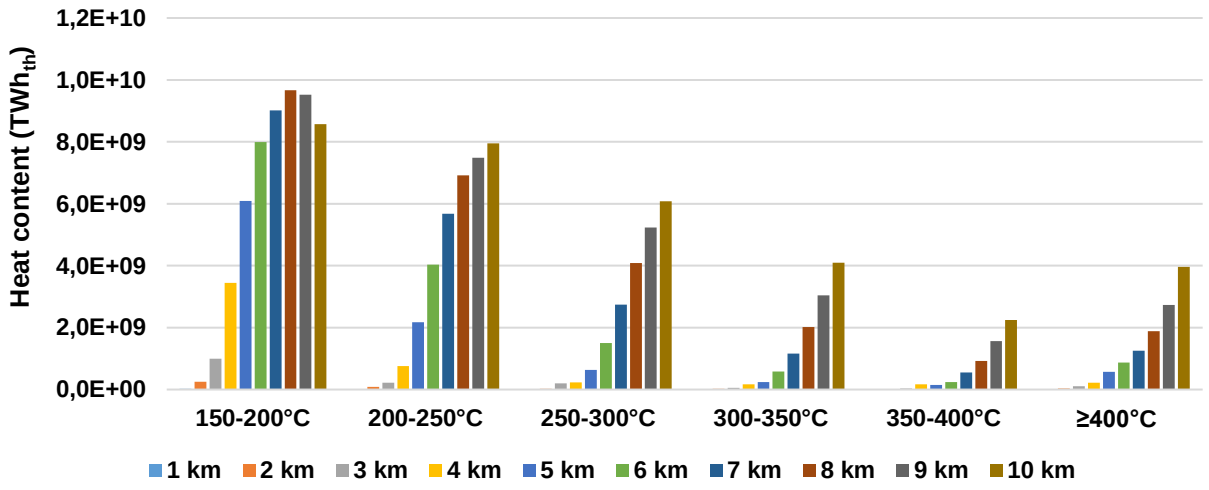

Fig. 4. Histograms of global EGS theoretical potential in terms of thermal energy (heat content) as a function of depth for the given temperature ranges.

After the estimation of recoverable heat from the reservoir, the heat has to be converted to usable energy. The energy can be either heat or electricity, as well as combination of both in the form of combined heat and power (CHP) plant. Theoretical potential of EGS power capacity, P_{theo} (MW_e), is derived using the Equation 5. Theoretical potential is an estimate of physically exploitable energy in a certain time. Therefore, this amount is set as the maximum energy that theoretically

can be extracted. However, only a fraction of theoretical potential can be accessible ultimately under the given technical, economic and sustainable constraints. This will be discussed in the following sections.

$$P_{theo} = H \cdot \frac{\eta_{th}}{Lifetime \cdot CF} \quad (5)$$

where *H* is the available heat content presented in Equation 3, η_{th} is the thermal efficiency, *Lifetime* is the lifetime of power plant, which is assumed to be 30 years (8760·30 = 262,800 hours) [33], and CF is the average geothermal capacity factor of 90% [67]. The heat value is converted from EJ to TWh using a conversion factor of 277.78.

The net thermal efficiency (η_{th}) is calculated using the Protocol's recommendation, as given in Equation 6. Two representative maps of net thermal efficiency at depths of 3 and 6 km are illustrated in the Supplementary Material (Figure S5).

$$\eta_{th} = 0.00052 \cdot T + 0.032 \quad (6)$$

where *T* is the mean fluid temperature and it is calculated based on the average of the initial rock temperature (T_z) and the base temperature (T_r), as provided in Equation 7.

$$T = \frac{(T_z + T_r)}{2} \quad (7)$$

3.3 Technical potential of EGS

It is clear that the determined theoretical potential for EGS cannot be entirely mined and utilised in any given location. There are multiple obstacles to extract the maximum theoretical potential of EGS systems. Considering the term "technical potential", several technical limitations will reduce the estimated theoretical potential considerably. In this context, as defined by Rybach [68], technical potential refers to the fraction of the theoretical potential that can be accessed and extracted with the current technology, while considering geographic, ecology, legal and regulatory restrictions. One of the technical limitations is related to land availability for EGS, referred to as *RA* in this manuscript, which can be classified as follows: 1) protected and conservation areas; 2) densely populated areas; 3) large lakes and reservoirs; 4) areas of high water stress. It is important to note that other technical parameters might restrict the land availability for maximum EGS

utilisation, such as militarised areas, specific topographic relief, and technical concerns about drilling technologies at great depths. However, only the four limitations listed above are considered to assess the EGS technical potential. It is assumed that other barriers might not have a substantial impact on the specified EGS locations. Nevertheless, at the time of preparation and installation of an EGS plant all the potential risks have to be probed deeply and studied. Some restrictions might change over time and should be re-evaluated when the field study is carried out for building the EGS plant. Population density, water stressed regions and costs of drilling and operation are some elements that can change with time.

The world database on protected areas are taken from the Protected Planet [69] and calibrated for the 1˚ grid cell. The database consists of 222,075 polygons, covering 245 countries and territories. The polygons with surface area of less than 1000 km^2 are excluded. The surface area of all the polygons located inside a grid cell is measured and its fraction to the total surface area of that cell is obtained. The gridded population density data with the resolution of 1˚×1˚ is gathered from the Center for International Earth Science Information Network (CIESIN) [70] for the year 2020. The large lakes and reservoirs data is obtained from [71] and compared with [72]. The surface area of the taken lakes are set to greater than 5000 km^2 to cover the main part of the grid cells. It is vital to mention that the wetlands and smaller water bodies have not been considered mainly due to their smaller sizes compared to a 1˚ cell size, which could result in exaggerated and inaccurate outcomes. It is recommended to account for wetlands and smaller water bodies in detailed regional studies to provide a more precise picture of the total exploitable geothermal potential. The global estimates of water stress centred for the year 2020 is collected from the World Resources Institute [73]. Among the climate scenarios, the Optimistic scenario for the year 2020 is selected. The polygons based database is converted to 1˚×1˚ resolution. Based on the projected change in water stress, the high (40-80%), extremely high (>80%), and arid and low water use areas are taken to quantify and visualise the restricted regions for geothermal development. The water stress map is an important factor for the EGS projects due to relatively high water withdrawals. It is investigated that EGS plants can consume between 0.3 and 0.7 gallons/kWh (≈1 - 3 m^3/MWh) [74,75], depending on the type of power plant. The respective maps of the four land access limitations for EGS development explained above are presented in the Supplementary Material (Figure S6).

It has been argued that the recoverable heat from the rock can be exploited for extended periods, with minimal thermal drawdown, if the EGS system is designed and operated attentively [18,33].

It is worthy to mention that the thermal drawdown is taken into account and restricted to proportional specified drop in the average rock temperature at a given depth. A maximum temperature drawdown of 10˚C [18,33] is assumed and the recoverability factor of temperature drawdown, R_{TD}, is determined as shown in Equation 8.

$$R_{TD} = \frac{10}{(T_z + T_r)} \tag{8}$$

Williams et al. [66] surveyed the recovery factor, *RF*, of thermal energy for an unexploited geothermal systems to range between 0.08 and 0.20. It is outlined that an identical probability can be considered over the entire range. For simplicity, a mean value of 0.14 is presumed.

Given all the aforementioned constraints, the technical potential of EGS power can be computed as given in Equation 9.

$$P_{tech} = P_{theo} \cdot (1 - RA) \cdot (1 - R_{TD}) \cdot RF \tag{9}$$

where P_{theo} is the theoretical potential of EGS for any given depth interval in a specific 1˚×1˚ cell. The other parameters have been introduced earlier. Both *RA* and R_{TD} are defined as values between 0 and 1. The *RA* is derived by overlapping different layers of land access limitations. Where a grid cell is fully covered by any of the layers or the combination of several layers, a value of 1 is assigned. This means there is no technical potential available for EGS in that particular cell. Eventually, the technical potential of EGS power is ascertained for 1 km depth interval, from 1 km to 10 km, and in 1˚ spatial resolution.

The derived maps for thermal energy based on the technical constraints are shown in Figure 5. The corresponding values for heat content globally are enumerated in Table 3 and visualised as histogram in Figure 6, respectively. The values of heat content are classified similar to Table 2. It can be observed that the distribution of heat content at various temperature ranges differs from the one presented in Figure 4. Several technical limitation factors applied reduce the amount of stored thermal energy and block some areas that were previously specified as high potential. This phenomenon results in considerably higher heat contents in the temperature range of 400˚C or higher, making it relatively comparable with the amount of heat at the range of 300-350˚C. As shown, there is a tremendous resource base at depths of 5 to 10 km in most of the temperature classes, and moderately lower resource at depths of 3 and 4 km.

EGS technical potential in terms of thermal energy at 1000 m depth (TWh_{th})

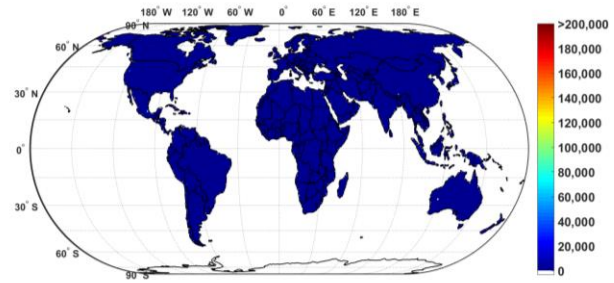

EGS technical potential in terms of thermal energy at 2000 m depth (TWh_{th})

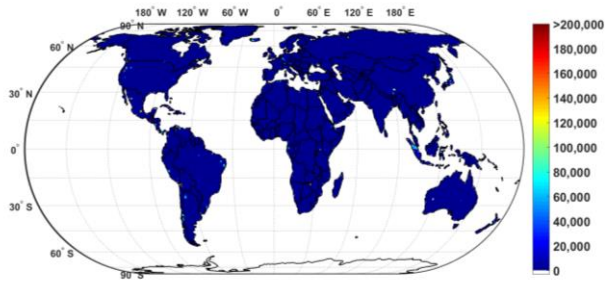

EGS technical potential in terms of thermal energy at 3000 m depth (TWh_{th})

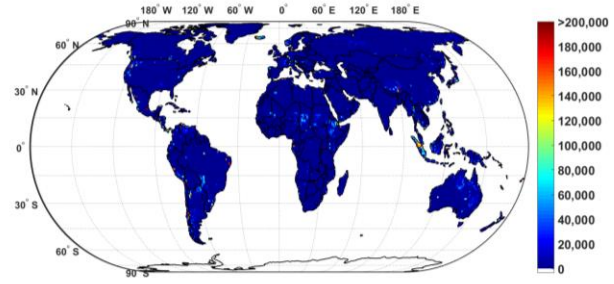

EGS technical potential in terms of thermal energy at 4000 m depth (TWh_{th})

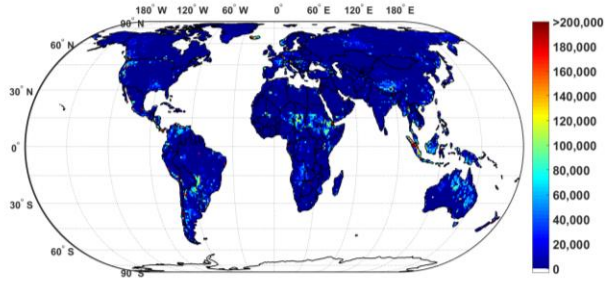

EGS technical potential in terms of thermal energy at 5000 m depth (TWh_{th})

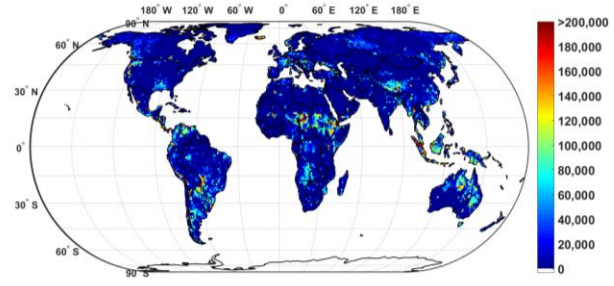

EGS technical potential in terms of thermal energy at 6000 m depth (TWh_{th})

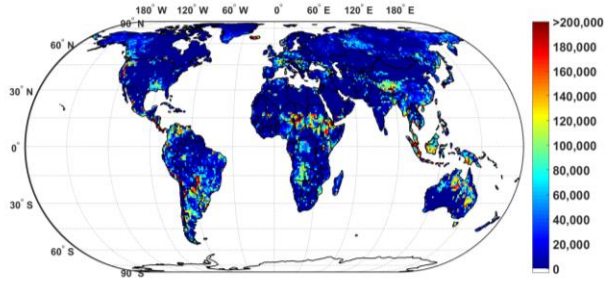

EGS technical potential in terms of thermal energy at 7000 m depth (TWh_{th})

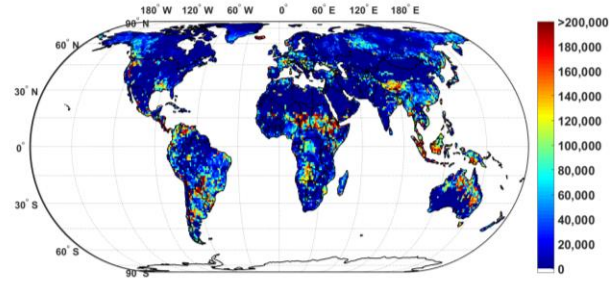

EGS technical potential in terms of thermal energy at 8000 m depth (TWh_{th})

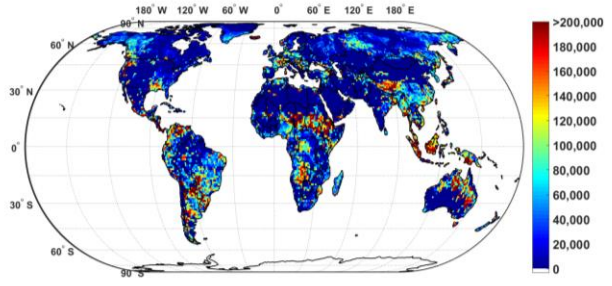

EGS technical potential in terms of thermal energy at 9000 m depth (TWh_{th})

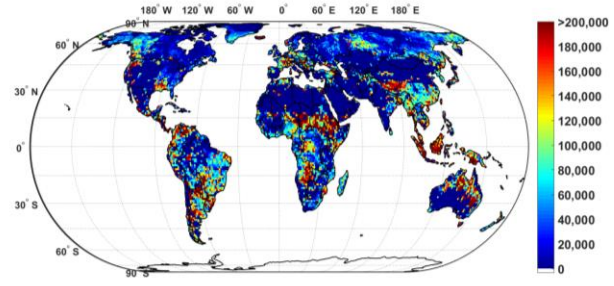

EGS technical potential in terms of thermal energy at 10000 m depth (TWh_{th})

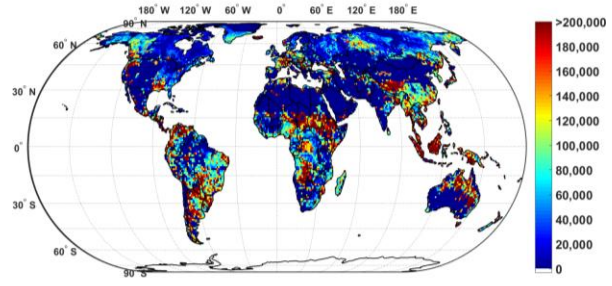

Fig. 5. Global EGS technical potential in terms of thermal energy at 1 km depth intervals.

Table 3. Available heat content estimated using technical constraints for 1 km depth intervals worldwide.

Heat content (TWh_{th})	150-200°C	200-250°C	250-300°C	300-350°C	350-400°C	≥400°C
1 km	3.7E+05	0.0E+00	1.5E+05	2.5E+05	0.0E+00	0.0E+00
2 km	3.2E+06	1.1E+06	5.9E+05	7.0E+05	4.8E+05	1.0E+06
3 km	1.0E+07	4.0E+06	4.6E+06	1.4E+06	6.8E+05	4.2E+06
4 km	4.0E+07	1.4E+07	4.9E+06	6.0E+06	3.6E+06	8.6E+06
5 km	8.2E+07	4.0E+07	1.4E+07	6.8E+06	4.8E+06	2.1E+07
6 km	1.1E+08	8.5E+07	3.5E+07	1.5E+07	8.1E+06	3.3E+07
7 km	1.3E+08	1.3E+08	7.0E+07	3.3E+07	1.6E+07	5.0E+07
8 km	1.4E+08	1.6E+08	1.1E+08	5.8E+07	2.9E+07	7.4E+07
9 km	1.5E+08	1.7E+08	1.5E+08	9.8E+07	5.1E+07	1.1E+08
10 km	1.4E+08	1.7E+08	1.8E+08	1.4E+08	7.5E+07	1.6E+08

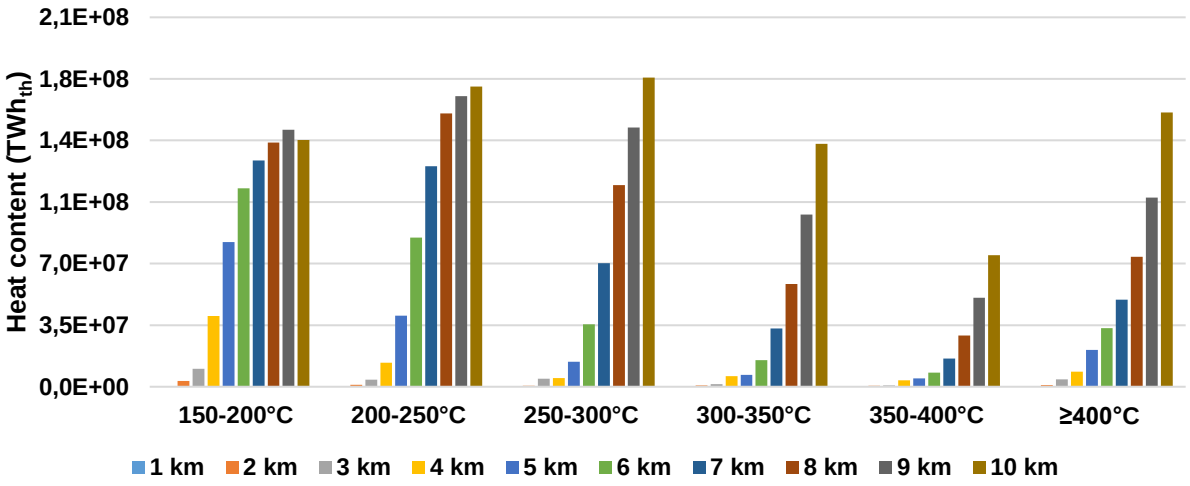

Fig. 6. Histograms of global EGS technical potential in terms of thermal energy (heat content), as a function of depth for the given temperature ranges.

3.4 Optimal economic potential of EGS

According to the Paris Agreement [76], Sustainable Development Goal (SDG) 7 [77] and the latest IPCC report [15], the amount of GHG emissions has to be reduced drastically to zero by 2050 to keep the temperature rise below 1.5˚C above pre-industrial levels. Increasing the share of variable renewable energy resources is crucial to decreasing the amount of GHG emissions and the

movement towards an entirely sustainable energy system. Therefore, the economic assumptions for the years 2030 and 2050 are applied to determine the role for geothermal energy in the global energy transition specified in the environmental frameworks. The economic assumptions from 2015 to 2050 are estimated in ten-year time steps and can be utilised to evaluate the optimum results for any given year. It is crucial to note that one of the main factors that can help enhance the geothermal energy installed capacity is the power plant cost per MW basis. If the costs of geothermal sites are not competitive enough with other renewable energy resources, in particular solar and wind energy, there would be less chance for geothermal energy to become a generator hub in the future energy system. Hence, the LCOE can help evaluate the optimal sites with the least-cost solution. The fundamental components and equations for estimating the cost for deep EGS are provided below. The detailed assumptions and equations can be found in the Supplementary Material.

The capital costs or capital expenditures (CAPEX) are calculated as the sum of the geothermal well drilling and completion costs ($C_{cap,well}$), the surface plant costs ($C_{cap,pp}$), the reservoir stimulation costs ($C_{cap,stim}$), the fluid distribution costs ($C_{cap,distr}$) and the resource exploration costs ($C_{cap,expl}$), as shown in Equation 10 [67]. In addition, a learning factor (LF) is applied to describe the specific technology learning.

$$\begin{aligned} CAPEX(z, T_r, T_z, \eta_{th}, W, q_0, k, t, y_0, y_f) \\ = \left(C_{cap,well}(z, T_z, q_0, k, t) \cdot n + \frac{C_{cap,pp}(T_r, T_z, \eta_{th}, W) \cdot W}{10^3} + C_{cap,stim} \right. \\ \left. + C_{cap,distr}(T_z) + C_{cap,expl}(z, T_z, q_0, k) \right) \cdot LF(y_0, y_f) \end{aligned} \quad (10)$$

where z is the depth, T_r is the base temperature, T_z is the temperature at depth z, η_{th} is the net thermal efficiency, W is the power plant capacity for the year t in MW, q_0 is the surface heat flow, k is the thermal conductivity, t is the year, n is the number of wells (production and injections wells), and LF is the learning factor calculated based on the reference cost year (y_0) and the future cost year (y_f), as shown in Equation S11.

A value of 2% of the estimated CAPEX is considered for the fixed operational expenditure (OPEX), according to the NREL [78] for both flash and binary plants and Carlsson et al. [79] for Organic Rankine Cycle (ORC) plants. The variable OPEX is set to zero.

Finally, the LCOE is calculated using the following Equation:

$$LCOE\left(z, T_r, T_z, \eta_{th}, W, q_0, k, t, y_0, y_f\right) = \frac{CAPEX(z, T_r, T_z, \eta_{th}, W, q_0, k, t, y_0, y_f) \cdot crf + OPEX_{fixed}(t)}{E(T_z, T_r, \eta_{th}, t)} + OPEX_{var}(t) \quad (11)$$

where $OPEX_{fixed}$ is the fixed OPEX in the year *t*, $OPEX_{var}$ is the variable OPEX in the year *t*, *crf* is the capital recovery factor. The average currency exchange rate is assumed at 1.2 USD/€ throughout the years, from 2015 to 2050.

In the next step, an optimum depth is determined by finding the first cell at each depth interval with temperature greater than or equal to 150˚C. Ultimately, there is a minimum LCOE in which all the EGS components are at their optimal points. Likewise, all other components including temperature-depth interval, available heat content, EGS technical potential in terms of power capacity, efficiency, CAPEX, and LCOE for the optimum depth are identified. Finding the optimum depth is crucial because the drilling costs, temperature and power plant efficiency increase with depth, and therefore the total power plant costs decrease. Eventually, there is a minimum LCOE in which all the involved components are at their optimal points. In fact, the LCOE declines since the amount of extractable heat, and thus electricity production, increases in the deeper depths, which outweighs the rise in drilling and surface plant costs. This explains the reduction in cost of electricity production per MWh. Whereas, in the shallower depths, where the drilling cost is cheaper, less heat content can be accessed and extracted, and consequently less electricity can be produced. Two sites in Iceland and the US are selected to illustrate this aspect in more details, as shown in Figure 7. It is likely that the most cost-effective and economical depth at a location would be advanced for deep EGS utilisation to increase the efficiency and profits of the plant. This would prevent the development of all the available resources in that location for the lifetime of the power plant, which might cause severe social and financial risks. The respective maps of all elements at the optimum depth are illustrated in Figure 8.

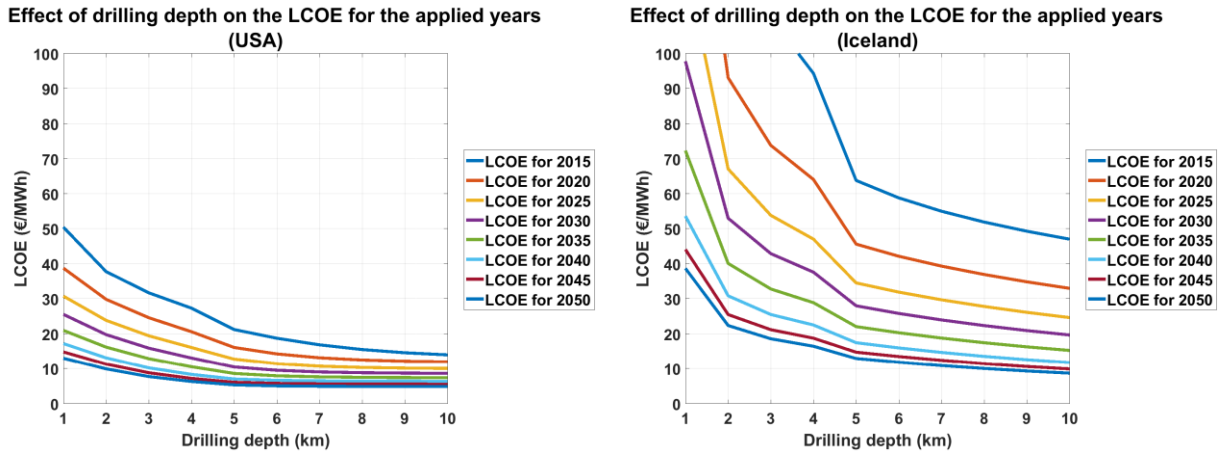

Fig. 7. Effects of drilling depth on the LCOE from 2015 to 2050 for the two assumed sites in the US (left) at 44°30'00" N/ 110°30'00" W and Iceland (right) at 64°30'00" N/ 20°30'00" W.

It is defined that all the optimum values for the LCOE higher than 150 €/MWh have to be excluded for economic reasons. This constraint further reduces the estimated technical potential of EGS. The final results consist of the theoretical potential, technical potential including and excluding economic constraint, technical potential excluding water stress, and technical potential excluding water stress and economic constraints for both thermal energy and power capacity, as shown in Tables 4 and 5. The results are presented for some selected countries as well as globally. The nominated countries represent the top ten most installed geothermal capacity as of today (Table 4) and the top ten countries with the highest identified EGS potential based on the economic constraints for the years 2030 and 2050 (Table 5). Some of the countries with the highest installed capacity as of today might be included in the top ten countries globally with the highest potential based on the given economic constraint. The results of all countries in the world are listed in The Supplementary Material (spreadsheet file 1).

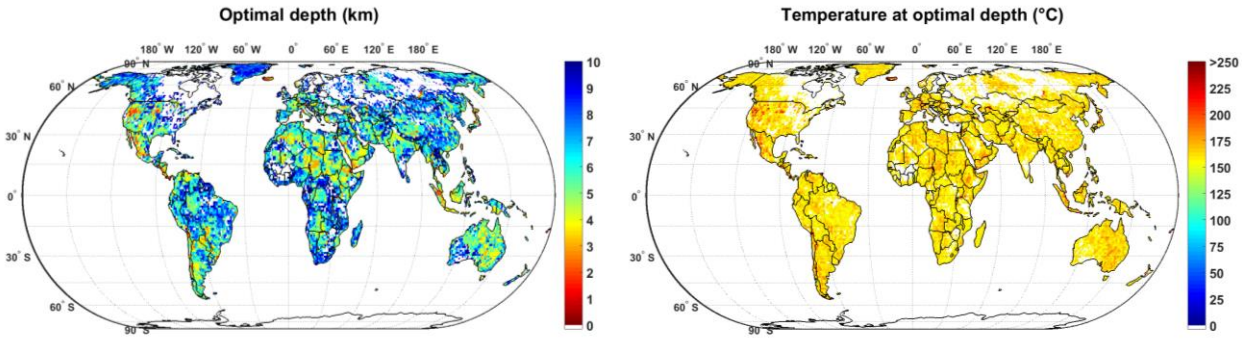

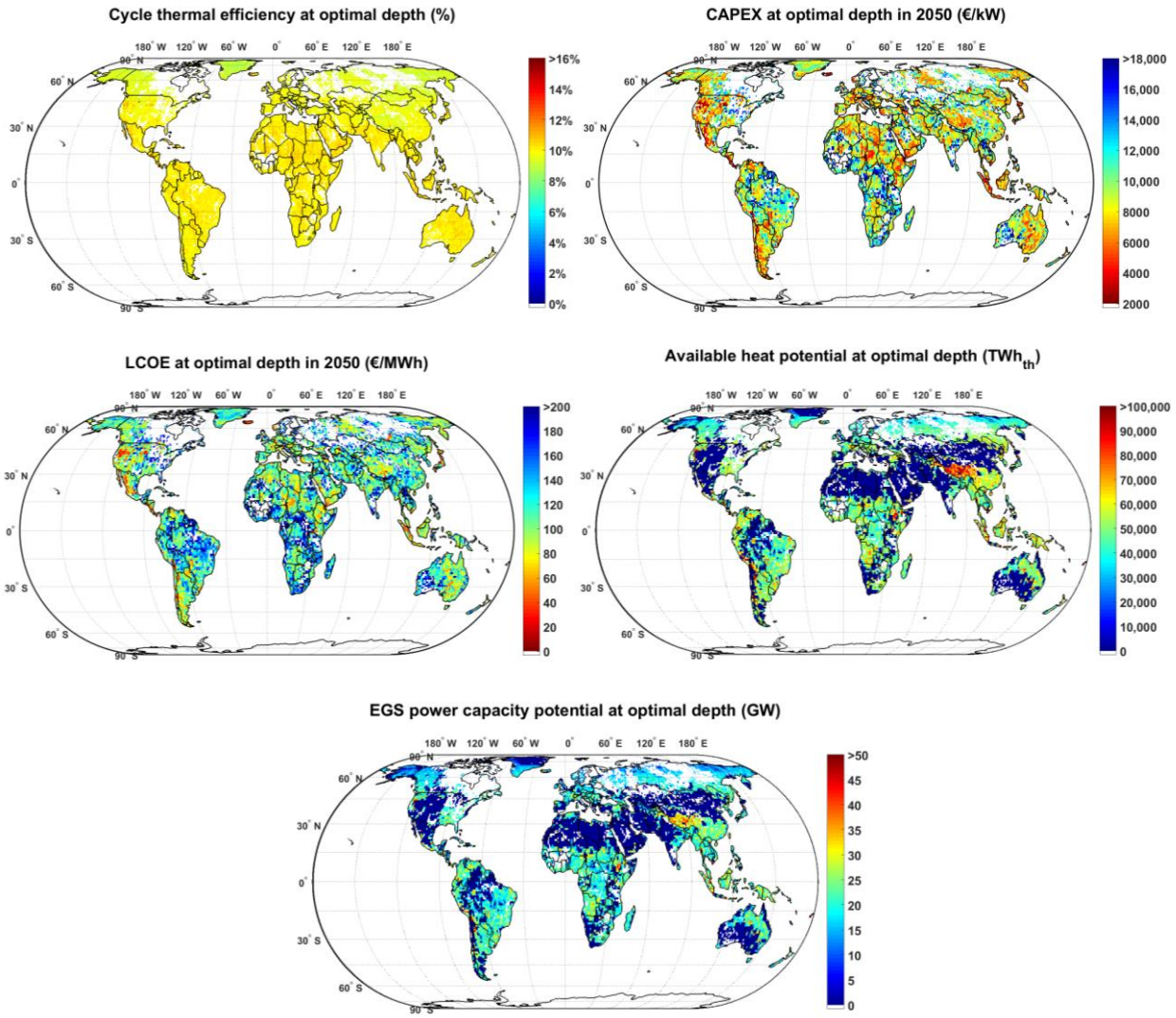

Fig. 8. Maps of all the components involved in estimation of stored thermal energy of the Earth's deep interior based on the identified optimum depth. The involved maps are: optimal depth (top left), and the following at optimal depth, temperature (top right), cycle thermal efficiency (centre left), CAPEX (centre right), LCOE (bottom left), available heat potential (bottom right), EGS power capacity potential (bottom).

A crucial decision-making factor for development of EGS projects is the production cost, i.e. how much energy can be produced at what cost level. Figure 9 presents an industrial cost curve for the LCOE as a function of EGS technical power capacity for the year 2050. The extractable capacities are classified in 5 €/MWh intervals, from 10-15 €/MWh to 95-100 €/MWh. The capacities with LCOE higher than 100 €/MWh are excluded. The findings indicate that around 4600 GW of EGS power capacity, or 36,300 TWh, could be installed at a cost of 50 €/MWh or lower. A greater

amount of 49,600 GW can be obtained in the LCOE range of 50 – 100 €/MWh. Detailed data on a country and global level is provided in the Supplementary Material (spreadsheet file 2). Further, the detailed EGS cost estimates for five exemplary sites are presented in the Supplementary Material (spreadsheet file 3).

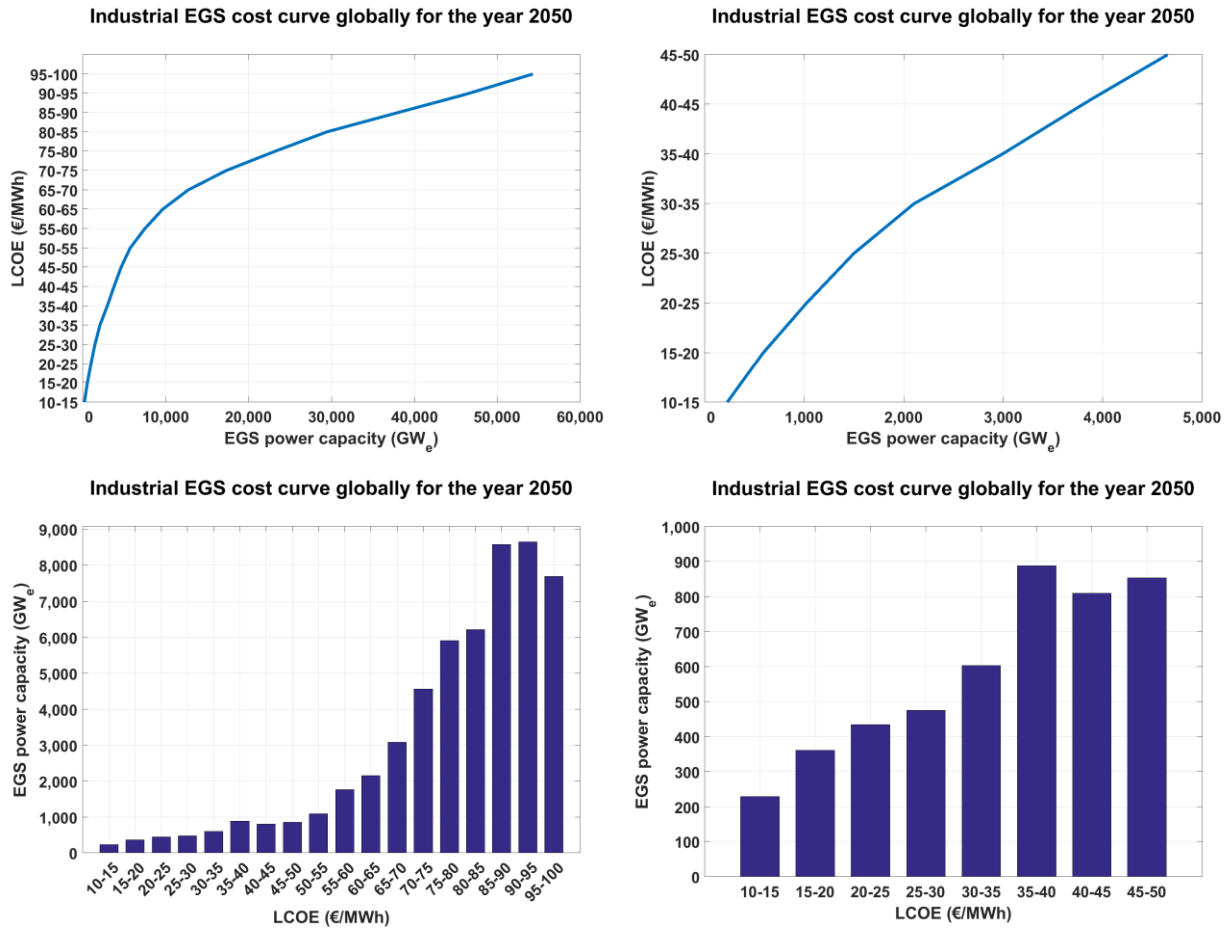

Fig. 9. Industrial cost curve for EGS, LCOE as a function of EGS technical power capacity, in a cumulative (top) and a spectral (right) format. The figures on the left are plotted for the LCOE range of 10 – 100 €/MWh and the ones on the right for the LCOE range of 10 – 50 €/MWh.

Table 4. The EGS optimal potential in terms of heat in place (thermal energy - TWh_{th}) and power capacity (GW_e) based on the optimum depth, with and without applied constraints, are presented for the selected countries as well as globally for the cost years of 2030 and 2050. Abbreviations: EC – economic constraint, WC – water stress constraint. Detailed data is presented for all countries in the Supplementary Material (spreadsheet file 1).

Countries	Heat in place (2030)	Heat in place (2050)	Heat in place excl. EC	Heat in place excl. WC (2030)	Heat in place excl. WC (2050)	Heat in place excl. EC & WC	EGS power capacity (2030)	EGS power capacity (2050)	EGS power excl. EC	EGS power excl. WC (2030)	EGS power excl. WC (2050)	EGS power excl. EC & WC
United States	723,218	13,944,465	17,614,246	3,948,448	30,848,755	36,953,041	337	5,774	7,272	1,772	12,914	15,401
Indonesia	1,181,980	7,517,474	7,715,525	1,181,980	7,901,857	8,099,908	533	3,275	3,359	533	3,447	3,531
Philippines	-	594,309	817,168	-	800,981	1,023,839	-	257	351	-	345	440
Turkey	139,470	1,655,745	1,906,501	280,553	3,546,782	4,029,964	61	686	789	121	1,480	1,677
New Zealand	103,422	855,652	1,086,641	103,422	855,652	1,086,641	49	361	455	49	361	455
Mexico	427,182	2,419,776	2,777,993	1,470,563	6,885,209	7,496,754	194	1,050	1,202	671	2,990	3,247
Italy	120,839	914,392	1,008,287	494,581	1,524,808	1,668,467	53	388	426	225	658	717
Iceland	688,138	723,337	723,337	688,138	723,337	723,337	312	325	325	312	325	325
Kenya	70,693	1,665,624	1,714,871	70,693	1,715,670	1,764,917	31	718	738	31	739	759
Japan	443,765	1,170,319	1,256,844	525,666	1,376,575	1,463,100	199	503	538	235	591	627
Global	12,848,300	258,200,637	319,323,033	20,395,458	394,036,567	481,088,048	5,823	108,064	133,145	9,218	165,623	201,403

Table 5. The EGS optimal potential in terms of heat in place (thermal energy - TWh_{th}) and power capacity (GW_e) based on the optimum depth, with and without applied constraints, are presented for the countries with the highest EGS technical power potential according to the economic constraint for the cost years of 2030 and 2050. Abbreviations: EC – economic constraint, WC – water stress constraint.

Countries	Heat in place	Heat in place excl. EC	Heat in place excl. WC	Heat in place excl. EC & WC	EGS power capacity	EGS power excl. EC	EGS power excl. WC	EGS power excl. EC & WC
2030								
Indonesia	1,181,980	7,715,525	1,181,980	8,099,908	533	3,359	533	3,531
Brazil	852,699	21,701,118	852,699	21,976,872	384	9,308	384	9,426
United States	723,218	17,614,246	3,948,448	36,953,041	337	7,272	1,772	15,401
Iceland	688,138	723,337	688,138	723,337	312	325	312	325
Chile	621,294	2,119,038	1,177,068	4,002,326	291	907	550	1,727
China	659,586	27,190,955	716,973	51,035,379	287	11,161	310	20,885
Argentina	467,831	10,617,014	619,630	14,717,955	208	4,482	271	6,206
Japan	443,765	1,256,844	525,666	1,463,100	199	538	235	627
Mexico	427,182	2,777,993	1,470,563	7,496,754	194	1,202	671	3,247
Canada	414,506	18,681,886	477,521	19,990,820	180	7,456	206	7,977
2050								
Russian Federation	44,217,398	55,753,854	47,009,618	59,265,077	17,621	22,131	18,754	23,551
China	24,028,592	27,190,955	43,817,052	51,035,379	9,882	11,161	17,975	20,885
Brazil	16,368,249	21,701,118	16,536,656	21,976,872	7,044	9,308	7,117	9,426
United States	13,944,465	17,614,246	30,848,755	36,953,041	5,774	7,272	12,914	15,401
Canada	14,329,316	18,681,886	15,274,804	19,990,820	5,742	7,456	6,119	7,977
Australia	12,755,514	13,989,778	22,548,209	26,775,994	5,524	6,043	9,734	11,509
Argentina	10,122,994	10,617,014	14,179,423	14,717,955	4,276	4,482	5,981	6,206
Indonesia	7,517,474	7,715,525	7,901,857	8,099,908	3,275	3,359	3,447	3,531
Greenland	7,839,170	8,559,025	7,839,170	8,559,025	3,018	3,291	3,018	3,291
Sudan	4,654,380	5,031,101	6,944,389	7,760,652	2,019	2,181	3,018	3,368

3.5 Sustainable potential of EGS

Both renewable and sustainable terms are widely used for various renewable energy sources, including geothermal energy. However, these two terms can be confusing. It is crucial to stress that the term renewable refers to the nature of an everlasting resource in human dimensions. The latter concerns how a resource is utilised and with what impacts on the environment and society [6]. Geothermal heat extraction is not similar to a mining process, since the extracted heat can be refurbished over time, albeit it might happen at slow rates. The required time for regeneration of geothermal resources depends on various factors, such as characteristics of the resource, type and size of the production system, and the rate of extraction. In general, lower extraction rates can ensure a relatively constant production over the lifetime of EGS systems. It has been stated that as long as a small fraction of the total geothermal technical potential, e.g. less than 10%, is utilised, geothermal energy can be treated as a sustainable resource [18]. Chamorro et al. [23] suggest a restrictive method to estimate the sustainable potential of EGS systems. The authors assumed that the sustainable potential is just the amount of energy that can be extracted at the same rate as it is captured by and generated within the same volume of rock. This proposed method is applied, with a slight modification where the land availability is considered, to estimate how much of the identified EGS power capacity can be produced sustainably, as expressed in Equation 12.

$$W_{sustain} = \left((q_{10000} \cdot SA_T \cdot \eta_{th}) + (A \cdot V_c \cdot \eta_{th})\right) \cdot (1 - RA) \quad (12)$$

where $W_{sustain}$ is the sustainable power plant capacity in W, q_{10000} is the heat flow at 10,000 m depth, obtained from Equation 13, and SA_T is the surface area at 10,000 m depth and temperature T (T > 150 C), η_{th} is the thermal efficiency as a function of resource temperature, A is the heat production, V_c is the volume of rock, and RA represents technical limitations related to land availability for EGS.

$$q_{10000} = q_0 - 10{,}000 \cdot A \quad (13)$$

where q_0 is the surface heat flow.

The global sustainable heat in place and power capacity are shown in Figure 10. The results on a country, regional and global level are presented in the Supplementary Material (spreadsheet file 1). The global EGS sustainable power capacity is around 256 GW, which is 0.2% of the estimated technical potential. The main parameters that result in the drastic reduction of sustainable potential

are the decrease in the amount of surface heat flow, excluding the impact of density and specific heat capacity of the rock and the temperature, albeit the temperature is indirectly considered through efficiency. This indicates that the sustainable extractable geothermal resources are by far less than the technical ones, even with the additional constraints considered for the technical potential estimate. Although utilising the sustainable power capacity might limit the contribution of geothermal energy in some parts of the world, there is still sufficient capacity to meet the increasing energy demand in the future based on an energy system with high shares of renewable energy resources.

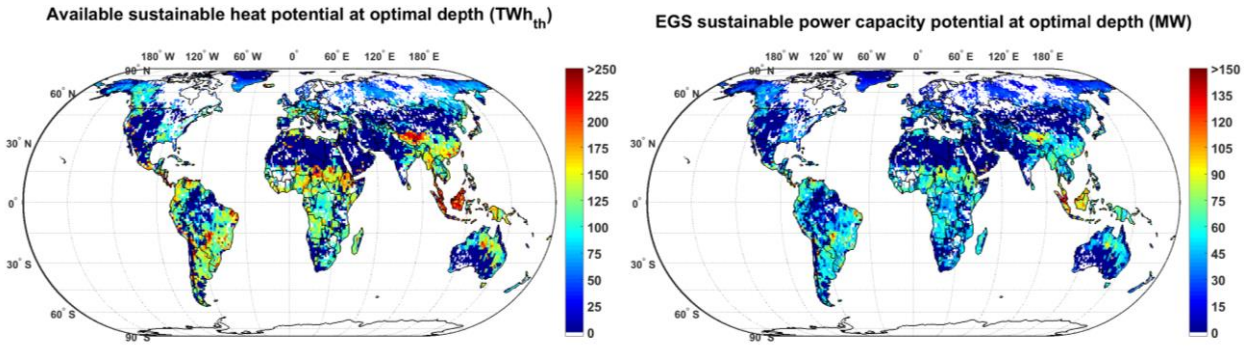

Fig. 10. Global available sustainable heat potential (left) and EGS sustainable power capacity potential (right) at optimal depth.

4. Discussion

4.1 Interpretation of the results

As shown in Tables 4 and 5, the EGS technical potential ($T_z \geq 150^{\circ}C$) at various depths for the considered cost years of 2030 and 2050 are given. These values are also compared with EGS technical potential without economic and water stress constraints. The economic assessment indicates the sensitivity of the available heat content at depth intervals, which is related to the costs of drilling. The results clearly reveal the significant impact of the LCOE reduction over time on the extractable thermal energy from the subsurface. Among all countries, Russia has the highest EGS power capacity potential, accounting for 16% of the total global capacity for the year 2050, whereas its contribution to the total global capacity is around 1% by 2030. This indicates that as the cost of EGS reduces gradually, more countries can integrate geothermal energy into their

energy mix. The other leading countries are China (9%), Brazil (7%), the US (5%), Canada (5%) and Australia (5%) by 2050, as presented in Table 5. The Philippines accounts for only 0.2% of the global EGS power capacity in 2050, even though it ranks third among the top ten countries in terms of geothermal installed capacity, with around 2 GW, as of today. That said, the Philippines has great potential to integrate geothermal energy into its energy mix with around 260 GW. The current estimate demonstrates that only one-fifth of the identified EGS technical potential is equivalent to the total final energy demand in the Philippines in 2017.

In terms of the economic constraint, the findings reveal that available heat in places is higher for the year 2050 compared to the year 2030. This can be explained by decreasing the geothermal well costs over time due to drilling technology improvement. With regards to thermal energy growth, Russia experiences the highest increase, followed by Greenland (20,564%), Australia (8929%), Angola (4595%), India (3726%) and China (3543%). The same trend can be observed for the case of the EGS power capacity. When the economic constraint is excluded from the results, one can see the EGS potential would increase even further. The global EGS power capacity decreases by 96% and 19% in comparison with the EGS including the economic constraint for the years 2030 and 2050, respectively. Regarding the water stress constraint, countries such as Saudi Arabia, Libya, Iran, Kazakhstan, Kyrgyzstan and Oman are impacted the most, by around 90% or more, due to high water stress [73] in those countries. It is crucial to point out that the required water for EGS is not only related to the power plant itself, but also to the fluid required to inject into the injection wells in order to extract the stored heat from beneath the surface. If only the EGS technical potential is considered excluding the economic and water stress constraints, a global geothermal power capacity of about 200 TW_e is expected, which is double the EGS power capacity in 2050 and 37 times larger than 2030 capacity including the constraints. The EGS development will help the energy transition occur in a more flexible and efficient manner. Even if only 13% of the EGS power capacity estimates for 2050 are developed, the energy recovered would be sufficient to cover the total global final energy demand in 2016 of around 111,130 TWh. Also, 19% of the EGS technical potential in 2050 can satisfy the total global primary energy demand (160,050 TWh) in 2016.

However, as explained earlier, not all the geothermal resource base can be utilised sustainably. Fast production rates that go beyond the long-term recharge rate can result in reservoir depletion, which drastically decreases or might even stop an economic production [6]. The purpose of

sustainable production of geothermal energy is to secure and sustain the production rates on the long run. The EGS sustainable power capacity is estimated to be only 19 GW by 2030, which increases up to 256 GW by 2050 globally. This amount soars when the constraints are excluded resulting in 96% and 45% increase for the years 2030 and 2050, respectively. The presented findings indicate that sustainable geothermal resource utilisation decreases the great potential of the EGS significantly across the world. The sustainable potential of EGS is still noticeable to be considered for the final energy mix of an entirely sustainable energy system.

As briefly mentioned in the Results section, the extracted geothermal heat in the EGS projects can be utilised as heat, electricity, or combination of both in terms of CHP plants. The Landau plant in Germany is a typical example of commercialised EGS-based CHP plants working based on the principle of the ORC plant. This plant has an electrical power capacity of over 3 MW_e (22 GWh_e/a) and heat capacity of 3 MW_{th} (9.2 GWh_{th}/a) [80,81]. The generated electricity is sufficient to supply up to 6000 households and the heat generation covers the demand of 1000 households. The preliminary use of extracted geothermal heat is for electricity production, using thermal water with a temperature of almost 160˚C, explaining the higher electricity generation than heat supply despite having almost the same capacity installed for both heat and power. The residual heat with a temperature of 70-80˚C is then fed into the district heating network [82,83]. It has been discussed that transferring heat over long distances increases the costs. Thus, it is more economical for heat consumers to be located nearby the plant, or the other way around, to have geothermal plants placed close to heat consumers. Geothermally generated heat and electricity from EGS-based CHP plants can secure the energy supply in both heat and power sectors in the future.

4.2 Validation and comparison of key findings

It is crucial to validate and verify the presented model and results to clarify the accuracy of the data and the conclusions drawn from the results. However, since EGS is still in its infancy and has not been widely developed and implemented across the world, validation with actual plants is restricted. Existing literature, in which the EGS potential in different regions has been estimated, is employed to verify the accuracy of the presented model and results. First, the results are compared with the European study [23] for EGS. A linear regression model is applied to find the linear fit and coefficient of determination for technical and sustainable power capacity estimate.

The findings reveal a high level of similarity between the two research pieces, which have been presented and discussed in the Supplementary Material (Section 2 and Figures S1 and S2). Second, research results are compared to values reported by Tester et al. [18] for the theoretical heat potential of geothermal resource-base in the US. The comparison between the two studies are given in the Supplementary Material (Section 2 and Figure S3). The validation shows that the coefficient of determination is at a high correlation value of 0.88, and the distribution of geothermal resources among states are in accordance with the findings in this study.

According to the IEA [84], geothermal energy can play a role in the future energy system by providing 3.5% of global electricity production and 3.9% of the total heat generation by 2050. It is expected that more than half of the projected geothermal increase (200 GW_e) comes from EGS projects, dominated by binary power generation technology. However, the feasibility of EGS development earlier than 2030 is found to be challenging and requires significantly higher research, development and deployment. The remaining half of the geothermal energy (200 GW) will come from conventional geothermal systems. According to the Geothermal Energy Association [85], the total global geothermal capacity is expected to reach around 18.4 GW by 2021. In case all countries follow their geothermal development goals and targets, a 32 GW of geothermal installed capacity is expected by the early 2030s. Stefansson [86] stated that the global technical potential of hydrothermal resources for electricity generation can be as high as 240 GW, considering a range of 50-2000 GW depending on the assumptions. Even if the maximum potential of conventional geothermal systems (2000 GW) would be deployed, the EGS technical potential for the cost year 2050 is about 50 times higher than that. This shows a great potential of EGS for the sustainable future energy system.

The results of geothermal resource base estimates for the continental US conducted by Tester et al. [18] and Blackwell et al. [19], excluding Alaska, Hawaii, and Yellowstone National Park, reveal that a total of 13,267,370 EJ ($3.7 \cdot 10^9$ TWh_{th}) can be exploited. This amount of thermal energy is almost 100 times higher than that presented in this study for the most optimistic case (available technical heat content without any constraints). It is worth noting that the technical constraints applied for both thermal energy and power capacity have not been considered in the mentioned studies. Augustine [20] studied the geothermal resource availability for both conventional hydrothermal and EGS in the US, using the minimum LCOE at an optimum depth. A deep EGS power capacity potential of 15,908 GW_e is drawn. The optimum reservoir depths are found to be

in a depth of 5 km or deeper, which is in line with the findings of current study. Likewise, Lopez et al. [21] assessed the EGS potential to be 4000 GW_e for the US, adopting the quantitative analysis of LCOE. Chamorro et al. [23] concluded that the EGS technical potential in Europe is as much as 6560 GW_e, for depths of 3-10 km and temperature of higher than 150˚C. This result is somewhat in correlation with the present research, as the total EGS technical potential of Chamorro et al. is approximately 7.8 times higher than the 2030 value and almost identical with the 2050 value (6465 GW_e), respectively, excluding Russian territories in Europe. They also applied the sustainable EGS potential, assuming that the removable heat from the geothermal resources are replaced on a similar time scale. The estimated sustainable EGS potential is 27 GW_e, excluding Russia, which is about 200 times less than the technical potential. At the same time, this value is in line with the findings in this study (21 GW_e). It is critical to consider the sustainable heat resources since once all the available heat is extracted, the EGS plant has to be decommissioned earlier than its actual lifetime. This then leads to significant financial risk in the projects. As a sustainable energy resource, the extracted heat for geothermal energy has to be continuously replaced by additional energy from deeper levels on comparable time scales. Using balanced and moderate production rates for EGS, by considering the local resource characteristics such as field size, natural or induced recharge rates, can secure the longevity of production and sustainability of the resource [6,87].

Limberger et al. [26] analysed not only the technical potential for Europe, but also the economic potential considering the LCOE based on three well cost models for the years 2020, 2030, and 2050. It is summarised that the economic potential ranges between 19-522 GW_e for the given cost years with LCOE varying between 50-300 €/MWh. A geothermal resource assessment conducted by Lee et al. [22] highlights that South Korea has a great geothermal potential, which lies between 16,700 and 101,000 EJ ($4.6 \cdot 10^5$ and $280 \cdot 10^5$ TWh_{th}), depending on the depth. Each of these studies acknowledge the difficulties and uncertainties associated with implementing such broad data analysis to determine the geothermal resource potential, mainly due to lack of thorough knowledge and experience. It is clear that using diverse assumptions, configurations and approaches result in varied outcomes. This reaffirms the requirement for detailed modelling, case studies, and field tests around the issue.

As the cost of renewable energy, in particular solar photovoltaic [88] and wind energy [89], and energy storage [90,91] have been decreased substantially in the last decade, it is expected that

renewable energy contributes to the majority of installed capacity in the years to come. A 100% renewable energy-based system is modelled for the power sector alone globally and the estimated average LCOE is found to be 52 €/MWh in 2050 [4]. In an energy system with all sectors integrated, the LCOE and the total levelised cost of energy are estimated at 53 €/MWh each by 2050 [1]. The industrial cost curve presented in the Results section depicts that the extractable potential of EGS is significant and this technology can be cost competitive with other renewable energy resources. At least a part of the 4600 GW of the EGS power capacity that corresponds to 36,300 TWh of electricity production, with the LCOE of between 10-50 €/MWh, can be used very beneficially in a fully sustainable energy system by 2050. This makes the EGS an attractive technology to integrate into the energy mix of a renewable-based energy system.

4.3 Limitations and uncertainties

While the great potential of geothermal resources is ubiquitous in the world, there are still several challenges that need to be addressed before the development of EGS projects. Sustainability concerns about developing geothermal resources is one of the rare aspects featured in literature. Numerous sustainability indicators are listed to better manage the negative impacts of geothermal developments such as natural hazards, land use, deforestation, water quantity and quality, and ecosystems [92,93]. Micro-earthquakes, due to induced seismicity in response to an injection, can cause damage to local infrastructures and facilities. The Geothermal Engineering Integrating Mitigation of Induced Seismicity in Reservoirs (GEISER) is co-funded by the European Commission to regulate the advances in EGS applications in Europe [94]. Furthermore, the US Department of Energy published a Protocol [95] for addressing induced seismicity associated with EGS projects. This Protocol summarises that with detailed study and technology development, the effects of induced seismicity can be better evaluated and managed. A study analysed the optimisation of EGS considering the minimum LCOE and reducing induced seismicity risk [96]. It was concluded that the optimal sites might shift away from the densely populated areas, especially areas with unsafe constructions and buildings, to mitigate the seismic risk. This results in additional costs, albeit the added costs are manageable.

A main limitation of this research is the required input data in a high spatial resolution in order to estimate temperature as a function of depth. Although a great effort is made to collect as much

data as possible for surface heat flow, it would be beneficial to get access to higher quality of heat flow measurements, detailed geological studies and modelling to provide results that are more accurate. The values for heat conductivity are taken based on lithological classifications. An average number is considered for each class that might contain more than one sample. However, thermal conductivity might vary even in each class since there are multiple samples that might have different thermal properties. Radiogenic heat production is expanded on a country basis, which means an identical value is given for the whole country. As discussed for the case of thermal conductivity, heat production might not be the same throughout a country. The model improvements for temperature estimation at various depths can be attained when the quality, quantity, and accessibility of geological information, rocks and core sampling, and borehole measurements improve noticeably. Regarding the technical constraints, for the protected areas, only surface areas of higher than 1000 km^2 are taken into consideration. This ignores some polygons that are located within small countries and islands. Likewise, wetlands and small water bodies have been excluded from the assessment, which needs to be diffused for more detailed and small-scale studies. Additionally, the costs of drilling might be much lower in areas with thousands of wells drilled than those with hard rocks. Areas with high-porosity sands filled with water at high temperature, high crustal radioactivity, low thermal conductivity, high heat flow, and other suitable circumstances are more favourable for large-scale EGS development. Another important aspect is identifying an appropriate geological formation for an EGS site. For instance, crystalline and porous rocks are discussed as suitable candidates [97], where the former has been widely used and tested, e.g. the Soultz-sous-Forêt geothermal field. This requires field studies with several rock samplings and respective laboratory exercises to determine the lithology of different layers beneath the surface. Detailed explorations and studies are of utmost importance to identify the locations with the highest temperature, but low data availability.

With regards to all the aforementioned factors, it should be noted that the database and respective maps provided in this article present the potential areas with more suitability for EGS projects. The results should not be directly adopted for selecting areas for EGS installation. It serves as an initial guide for further investigation of local studies and designating favourable sites for EGS investments. The presented maps give a guideline for a rough estimate of the total exploitable heat from the Earth's interior and potential electricity that can be produced during the given lifetime of power plant and based on the underlying assumptions. The temperature at depth maps provide a

first order of estimate of the investment needed to exploit the resource. This information is useful and presented in a simple form that experts, project planners and decision-makers can employ for ranking the potential areas. Geothermal resource evaluation in this study is built on generally available and widely used data, equations and information, mainly inspired by the Protocol [33]. However, there are several critical conditions needed to be considered and addressed for a successful extraction of geothermal resources. These include, but not limited to, access to the borehole data and pumping results on a broad scale, which is currently only restricted to specific areas. Moreover, lithological formation and permeability of the rocks may vary underground over several orders of magnitude. Despite the selection of methods for quantifying resources, the amount of energy that can be eventually extracted is related to the development, optimisation and deployment of exploitation technology, as well as countries' policies and strategies.

5. Conclusions

With the growing demand of renewable energy and necessity for a rapid energy transition, the need to determine the maximum potential of renewable energy becomes increasingly important. Geothermal energy is a renewable energy resource that has great potential to help accelerate the shares of renewable energy in the energy mix. The conventional geothermal power system, hydrothermal, has been commercialised for a very long time. However, development of the emerging geothermal technology, EGS, has been limited to certain areas. This study presents an estimation of the technical, optimal economic and sustainable potential for the EGS on 1˚×1˚ spatial resolution globally. Temperature as a function of depth is modelled from 1 km to 10 km beneath the Earth's surface. To do so, a series of input data are primarily obtained from various resources, such as surface heat flow, thermal conductivity, radiogenic heat production, and surface ambient temperature. The collected data is then employed to estimate temperature at depth intervals. Next, the EGS theoretical and technical potential is attained. Finally, the optimum depth at temperature ≥150˚C is identified and the respective optimal economic potential components based on the given data and assumptions are obtained. The data is presented in 5-year time intervals, from 2015 to 2050. Further, in order to secure the sustainable production of geothermal energy over the long term, a method is applied to measure the sustainable geothermal resource base.

The global EGS optimal economic potential in terms of power capacity is found to be around 6 and 108 TW_e for the cost years of 2030 and 2050, respectively. Among all countries, Russia and China have the greatest EGS potential by 16% and 9% of total global capacity for the year 2050, respectively, followed by Brazil, the US, Canada and Australia. In the most optimistic scenario and without considering any constraints, such as cost and water stress, the global exploitable EGS potential is found to be about 200 TW_e, or $480 \cdot 10^6$ TWh_{th}. The economic constraint excludes the optimum values with LCOE higher than 150 €/MWh. This constraint is applied due to rapid cost reduction of other renewable energy resources, such as solar and wind energy. Nevertheless, the contribution of hybrid renewable energy systems provides security of energy supply as well as further flexibility into the energy system. If the full technical potential of EGS was implemented by 2050, the amount of electricity production from geothermal energy would be roughly 5 times higher than the total global primary energy demand in 2016. Additionally, the provided sustainable potential of EGS is approximately 256 GW_e in 2050, accounting for just 0.2% of the technical potential globally. That said, the sustainable potential of EGS is still noticeable to consider for the energy mix of an entirely sustainable energy system in the years to come. Moreover, an industrial cost curve is developed for the LCOE as a function of EGS technical power capacity in 5 €/MWh intervals, from 10-15 €/MWh to 95-100 €/MWh. The findings reveal that roughly 4600 GW of EGS power capacity can be built at a cost of 50 €/MWh or lower. A greater amount of 49,600 GW can be obtained in the LCOE range of 50 – 100 €/MWh.

It is vital to note that there are gaps in the data assumptions used for this research, mainly due to large-scale analysis and limited data availability. By filling the data gaps through small-scale and local studies, the model presented can estimate the EGS technical and sustainable potential more accurately. It is vital to emphasise that preceding the selection of a drilling site or EGS installation, a thorough analysis is imperative before any decision is made. This includes geological evaluation, tectonic settings, environmental impact assessment, potential induced micro-seismicity, field study and rock sampling. This will help policy-makers and governments to better assess the potential of geothermal energy in their countries to meet the increasing energy demand in the decades to come.

Conflicts of interest

There are no conflicts of interest to declare.

Acknowledgment

The authors gratefully acknowledge the public financing of Tekes, the Finnish Funding Agency for Innovation, for the 'Neo-Carbon Energy' project under the number 40101/14. The authors would like to thank Upeksha Caldera for proofreading. Also, the authors express their gratitude to the thorough review of anonymous reviewers.

References

[1] Ram M, Bogdanov D, Aghahosseini A, Gulagi A, Oyewo AS, Child M, et al. Global Energy System based on 100% Renewable Energy – Power, Heat, Transport and Desalination Sectors. Lappeenranta, Berlin: Study by Lappeenranta University of Technology and Energy Watch Group; 2019. http://energywatchgroup.org/wp-content/uploads/2017/11/Full-Study-100-Renewable-Energy-Worldwide-Power-Sector.pdf.

[2] Jacobson MZ, Delucchi MA, Cameron MA, Mathiesen B V. Matching demand with supply at low cost in 139 countries among 20 world regions with 100% intermittent wind, water, and sunlight (WWS) for all purposes. Renew Energy 2018;123:236–48. https://doi.org/10.1016/J.RENENE.2018.02.009.

[3] Teske S. Achieving the Paris Climate Agreement Goals: Global and Regional 100% Renewable Energy Scenarios with Non-energy GHG Pathways for +1.5°C and +2°C. Springer International Publishing; 2019. https://doi.org/10.1007/978-3-030-05843-2.

[4] Bogdanov D, Farfan J, Sadovskaia K, Aghahosseini A, Child M, Gulagi A, et al. Radical transformation pathway towards sustainable electricity via evolutionary steps. Nat Commun 2019;10:1077. https://doi.org/10.1038/s41467-019-08855-1.

[5] Huenges E. Geothermal Energy Systems: Exploration, Development, and Utilization. Weinheim: Wiley-VCH Verlag GmbH & Co. KGaA; 2010. https://doi.org/10.1002/9783527630479.

[6] Rybach L, Mongillo M. Geothermal Sustainability - A Review with Identified Research Needs. GRC Trans 2006;30:1083–90.

[7] Think GeoEnergy. Global geothermal power generation capacity reaches 14,600 MW at year end 2018 2019. http://www.thinkgeoenergy.com/global-geothermal-power-generation-capacity-reaches-14600-mw-at-year-end-2018/ (accessed June 24, 2019).

[8] [REN21] - Renewable Energy Policy Network for the 21st Century. Renewables 2019 - Global Status Report. Paris: REN21 Secretariat; 2019. http://www.ren21.net/gsr-2019/.

[9] [IEA] - International Energy Agency. Market Report Series: Renewables 2018. Paris: IEA Publishing; 2018. https://webstore.iea.org/market-report-series-renewables-2018.

[10] Lund JW, Boyd TL. Direct utilization of geothermal energy 2015 worldwide review. Geothermics 2016;60:66–93. https://doi.org/10.1016/j.geothermics.2015.11.004.

[11] Soltani M, Moradi Kashkooli F, Dehghani-Sanij AR, Nokhosteen A, Ahmadi-Joughi A, Gharali K, et al. A comprehensive review of geothermal energy evolution and development. Int J Green Energy 2019;16:971–1009. https://doi.org/10.1080/15435075.2019.1650047.

[12] Self SJ, Reddy B V., Rosen MA. Geothermal heat pump systems: Status review and comparison with other heating options. Appl Energy 2013;101:341–8. https://doi.org/10.1016/j.apenergy.2012.01.048.
[13] Soltani M, M. Kashkooli F, Dehghani-Sanij AR, Kazemi AR, Bordbar N, Farshchi MJ, et al. A comprehensive study of geothermal heating and cooling systems. Sustain Cities Soc 2019;44:793–818. https://doi.org/10.1016/j.scs.2018.09.036.
[14] Sanner B. Geothermal Systems and Technologies: Shallow Geothermal Systems. Geothermal Communities; n.d. https://geothermalcommunities.eu/assets/elearning/6.22.Shallow Geothermal SYstems.pdf.
[15] IPCC. Global Warming of 1.5 °C. Geneva: Intergovernmental Panel on Climate Change; 2018. http://ipcc.ch/report/sr15/.
[16] Rybach L. CO2 Emission Mitigation by Geothermal Development - Especially with Geothermal Heat Pumps. World Geotherm. Congr., Bali: 25-29 April; 2010.
[17] Menberg K, Pfister S, Blum P, Bayer P. A matter of meters: State of the art in the life cycle assessment of enhanced geothermal systems. Energy Environ Sci 2016;9:2720–43. https://doi.org/10.1039/c6ee01043a.
[18] Tester JW, Anderson BJ, Batchelor AS, Blackwell DD, DiPippo R, Drake EM, et al. The Future of Geothermal Energy: Impact of Enhanced Geothermal Systems (EGS) on the United States in the 21st Century. Cambridge, Massachusetts: 2006. https://doi.org/10.1016/j.jbusres.2015.10.046.
[19] Blackwell DD, Negraru PT, Richards MC. Assessment of the enhanced geothermal system resource base of the United States. Nat Resour Res 2006;15:283–308. https://doi.org/10.1007/s11053-007-9028-7.
[20] Augustine C. Updated U.S. Geothermal Supply Characterization and Representation for Market Penetration Model Input. Golden, CO: National Renewable Energy Laboratory, NREL/TP-6A20-47459; 2011. https://www.nrel.gov/docs/fy12osti/47459.pdf.
[21] Lopez A, Roberts B, Heimiller D, Blair N, Porro G. U.S. Renewable Energy Technical Potentials: A GIS-Based Analysis. Golden, CO: National Renewable Energy Laboratory, NREL/TP-6A20-51946; 2012. https://www.nrel.gov/docs/fy12osti/51946.pdf.
[22] Lee Y, Park S, Kim J, Kim HC, Koo M-H. Geothermal resource assessment in Korea. Renew Sustain Energy Rev 2010;14:2392–400. https://doi.org/10.1016/J.RSER.2010.05.003.
[23] Chamorro CR, García-Cuesta JL, Mondéjar ME, Pérez-Madrazo A. Enhanced geothermal systems in Europe: An estimation and comparison of the technical and sustainable potentials. Energy 2014;65:250–63. https://doi.org/10.1016/J.ENERGY.2013.11.078.
[24] Chamorro CR, García-Cuesta JL, Mondéjar ME, Linares MM. An estimation of the enhanced geothermal systems potential for the Iberian Peninsula. Renew Energy 2014;66:1–14. https://doi.org/10.1016/J.RENENE.2013.11.065.
[25] Jain C, Vogt C, Clauser C. Maximum potential for geothermal power in Germany based on engineered geothermal systems. Geotherm Energy 2015;3:1–20. https://doi.org/10.1186/s40517-015-0033-5.
[26] Limberger J, Calcagno P, Manzella A, Trumpy E, Boxem T, Pluymaekers MPD, et al. Assessing the prospective resource base for enhanced geothermal systems in Europe. Geotherm Energy Sci 2014;2:55–71. https://doi.org/10.5194/gtes-2-55-2014.
[27] Busby J, Terrington R. Assessment of the resource base for engineered geothermal systems in Great Britain. Geotherm Energy 2017;5. https://doi.org/10.1186/s40517-017-0066-z.

[28] Gerber L, Maréchal F. Environomic optimal configurations of geothermal energy conversion systems: Application to the future construction of Enhanced Geothermal Systems in Switzerland. Energy 2012;45:908–23. https://doi.org/10.1016/j.energy.2012.06.068.
[29] Hofmann H, Weides S, Babadagli T, Zimmermann G, Moeck I, Majorowicz J, et al. Potential for enhanced geothermal systems in Alberta, Canada. Energy 2014;69:578–91. https://doi.org/10.1016/j.energy.2014.03.053.
[30] Zhu J, Hu K, Lu X, Huang X, Liu K, Wu X. A review of geothermal energy resources, development, and applications in China: Current status and prospects. Energy 2015;93:466–83. https://doi.org/10.1016/j.energy.2015.08.098.
[31] Wang G, Li K, Wen D, Lin W, Lin L, Liu Z, et al. Assessment of Geothermal Resources in China. Thirty-Eighth Work. Geotherm. Reserv. Eng., Stanford University, Stanford, California: SGP-TR-198; 2013.
[32] Xia L, Zhang Y. An overview of world geothermal power generation and a case study on China—The resource and market perspective. Renew Sustain Energy Rev 2019;112:411–23. https://doi.org/10.1016/j.rser.2019.05.058.
[33] Beardsmore G, Rybach L, Blackwell D, Baron C. A Protocol for Estimating and Mapping Global EGS Potential. Geotherm Resour Counc Trans 2010;34:301–12.
[34] QGIS Development Team. QGIS geographic information system 2019.
[35] The MathWorks. MATLAB and Statistics Toolbox Release 2016b. Inc Natick 2016.
[36] [IHFC] - International Heat Flow Commission. Global heat flow 2008. http://www.geophysik.rwth-aachen.de/IHFC/heatflow.html (accessed January 6, 2019).
[37] [AAPG] - American Association of Petroleum Geologists. Global Heat Flow Database 2019. http://www.datapages.com/gis-map-publishing-program/gis-open-files/global-framework/global-heat-flow-database (accessed January 10, 2019).
[38] Pollack HN, Hurter SJ, Johnson JR. Heat flow from the Earth's interior: Analysis of the global data set. Rev Geophys 1993;31:267–80. https://doi.org/10.1029/93RG01249.
[39] Cermák V, Rybach L. Terrestrial Heat Flow in Europe. Berlin, Heidelberg, New York: Springer-Verlag; 1979.
[40] Majorowicz J, Wybraniec S. New terrestrial heat flow map of Europe after regional paleoclimatic correction application. Int J Earth Sci 2011;100:881–7. https://doi.org/10.1007/s00531-010-0526-1.
[41] O'Regan M, Preto P, Stranne C, Jakobsson M, Koshurnikov A. Surface heat flow measurements from the East Siberian continental slope and southern Lomonosov Ridge, Arctic Ocean. Geochemistry, Geophys Geosystems 2016;17:1608–22. https://doi.org/10.1002/2016GC006284.
[42] Le Gal V, Lucazeau F, Cannat M, Poort J, Monnin C, Battani A, et al. Heat flow, morphology, pore fluids and hydrothermal circulation in a typical Mid-Atlantic Ridge flank near Oceanographer Fracture Zone. Earth Planet Sci Lett 2018;482:423–33. https://doi.org/10.1016/J.EPSL.2017.11.035.
[43] Erkan K. Crustal heat flow measurements in western Anatolia from borehole equilibrium temperatures. Solid Earth 2015;6:103–13. https://doi.org/10.5194/se-6-103-2015.
[44] Hamza VM, Eston SM, Araujo RLC. Geothermal energy prospects in Brazil: A preliminary analysis. Pure Appl Geophys PAGEOPH 1978;117:180–95. https://doi.org/10.1007/BF00879745.
[45] Mono JA, Ndougsa-Mbarga T, Tarek Y, Ngoh JD, Owono Amougou OUI. Estimation of

Curie-point depths, geothermal gradients and near-surface heat flow from spectral analysis of aeromagnetic data in the Loum – Minta area (Centre-East Cameroon). Egypt J Pet 2018;27:1291–9. https://doi.org/10.1016/J.EJPE.2018.07.002.
[46] Omokenu EG, Nwosu1 LI. Spatial Variation Modeling of Geothermal Gradient and Heat Flow in Eastern Parts of Niger Delta Sedimentary Basin, Nigeria. Phys Sci Int J 2017;14.
[47] Evans TR. Terrestrial Heat Flow Studies in Eastern Africa and the North Sea. Imperial College London, 1975.
[48] Khojamli A, Ardejani FD, Moradzadeh A, Kalate AN, Kahoo AR, Porkhial S. Estimation of Curie point depths and heat flow from Ardebil province, Iran, using aeromagnetic data. Arab J Geosci 2016;9:383. https://doi.org/10.1007/s12517-016-2400-3.
[49] Kim HC, Lee Y. Heat flow in the Republic of Korea. J Geophys Res 2007;112:B05413. https://doi.org/10.1029/2006JB004266.
[50] [SEARG] - Southeast Asia Research Group. SE Asia Heatflow Databse 2016. http://searg.rhul.ac.uk/current-research/heat-flow/.
[51] Prol-Ledesma RM, Carrillo-de la Cruz JL, Torres-Vera MA, Membrillo-Abad AS, Espinoza-Ojeda OM. Heat flow map and geothermal resources in Mexico. Terra Digit 2018;2:1–15.
[52] Prol-Ledesma RM, Morán-Zenteno DJ. Heat flow and geothermal provinces in Mexico. Geothermics 2019;78:183–200. https://doi.org/10.1016/J.GEOTHERMICS.2018.12.009.
[53] Hamza VM, Muñoz M. Heat flow map of South America. Geothermics 1996;25:599–646. https://doi.org/10.1016/S0375-6505(96)00025-9.
[54] Cermak V, Rybach L. Terrestrial Heat Flow and the Lithosphere Structure. Berlin, Heidelberg: Springer-Verlag Berlin Heidelberg; 1991. https://doi.org/10.1007/978-3-642-75582-8.
[55] National Centers for Environmental Information. Borehole Datasets 2019. https://www.ncdc.noaa.gov/data-access/paleoclimatology-data/datasets/borehole (accessed January 28, 2019).
[56] Goutorbe B, Poort J, Lucazeau F, Raillard S. Global heat flow trends resolved from multiple geological and geophysical proxies. Geophys J Int 2011;187:1405–19. https://doi.org/10.1111/j.1365-246X.2011.05228.x.
[57] Davies JH. Global map of solid Earth surface heat flow. Geochemistry, Geophys Geosystems 2013;14:4608–22. https://doi.org/10.1002/ggge.20271.
[58] Hartmann J, Moosdorf N. The new global lithological map database GLiM: A representation of rock properties at the Earth surface. Geochemistry, Geophys Geosystems 2012;13:1–37. https://doi.org/10.1029/2012GC004370.
[59] Blackwell DD, Steele JL. Thermal Conductivity of Sedimentary Rocks: Measurement and Significance. Therm. Hist. Sediment. Basins, New York, NY: Springer New York; 1989, p. 13–36. https://doi.org/10.1007/978-1-4612-3492-0_2.
[60] Gallagher K, Ramsdale M, Lonergan L, Morrow D. The role of thermal conductivity measurements in modelling thermal histories in sedimentary basins. Mar Pet Geol 1997;14:201–14. https://doi.org/10.1016/S0264-8172(96)00068-2.
[61] Vosteen H-D, Schellschmidt R. Influence of temperature on thermal conductivity, thermal capacity and thermal diffusivity for different types of rock. Phys Chem Earth, Parts A/B/C 2003;28:499–509. https://doi.org/10.1016/S1474-7065(03)00069-X.
[62] Arafin S, Singh RN. Thermal and Transport Properties of Mafic and Ultramafic Rocks of Oman Ophiolite. SQU J Sci 2016;21:69–81.

[63] Haenel R, Stegena L, Rybach L. Handbook of Terrestrial Heat-Flow Density Determination: with Guidelines and Recommendations of the International Heat-Flow Commission. Springer Netherlands; 1988. https://doi.org/10.1007/978-94-009-2847-3.
[64] Stackhouse et al. NASA Prediction Of Worldwide Energy Resources (POWER), Surface Meteorology and Solar Energy (SSE) 2018. https://power.larc.nasa.gov/ (accessed December 10, 2018).
[65] Gutro R. 2005 Warmest Year in Over a Century 2006. https://www.nasa.gov/vision/earth/environment/2005_warmest.html (accessed July 2, 2019).
[66] Williams CF, Reed MJ, Mariner RH. A review of methods applied by the U.S. Geological Survey in the assessment of identified geothermal resources. Reston, Virginia: U.S. Geological Survey, Open-File Report 2008-1296; 2008. https://pubs.usgs.gov/of/2008/1296/.
[67] Beckers KF, Lukawski MZ, Anderson BJ, Moore MC, Tester JW. Levelized costs of electricity and direct-use heat from Enhanced Geothermal Systems. J Renew Sustain Energy 2014;6:013141. https://doi.org/10.1063/1.4865575.
[68] Rybach L. "The Future of Geothermal Energy" and Its Challenges. World Geotherm. Congr., 2010.
[69] UNEP-WCMC. Protected areas map of the world 2019. https://www.protectedplanet.net/ (accessed June 13, 2019).
[70] Center for International Earth Science Information Network - CIESIN - Columbia University. Gridded Population of the World, Version 4 (GPWv4): Population Density Adjusted to Match 2015 Revision UN WPP Country Totals, Revision 11 2018. https://doi.org/10.7927/H4F47M65 (accessed May 22, 2019).
[71] Tapiquén CEP. World lakes 2015. http://tapiquen-sig.jimdo.com (accessed May 24, 2019).
[72] Lehner B, Döll P. Development and validation of a global database of lakes, reservoirs and wetlands. J Hydrol 2004;296:1–22. https://doi.org/10.1016/J.JHYDROL.2004.03.028.
[73] Luck M, Landis M, Gassert F. Aqueduct Water Stress Projections: Decadal Projections of Water Supply and Demand Using CMIP5 GCMs, Technical Note. Washington, D.C.: World Resources Institute; 2015. http://www.wri.org/publication/aqueduct-water-stress-projections.
[74] Clark C, Harto C, Sullivan J, Wang M. Water Use in the Development and Operation of Geothermal Power Plants. Lemont, IL: Argonne National Laboratory, Environmental Science Division, ANL/EVC/R-10/5; 2011. http://www.evs.anl.gov/downloads/ANL_EVS_R-10_5.pdf.
[75] Macknick J, Newmark R, Heath G, Hallett KC. Operational water consumption and withdrawal factors for electricity generating technologies: a review of existing literature. Environ Res Lett 2012;7:045802. https://doi.org/10.1088/1748-9326/7/4/045802.
[76] [UNFCCC] – United Nations Framework Convention on Climate Change. Adoption of the Paris Agreement - Proposal by the President. Paris: UNFCCC; 2015. https://unfccc.int/resource/docs/2015/cop21/eng/l09.pdf (accessed June 22, 2016).
[77] United Nations. Sustainable development goals 2015. http://www.un.org/sustainabledevelopment/sustainable-development-goals/.
[78] [NREL] - National Renewable Energy Laboratory. 2018 Annual Technology Baseline 2018. https://atb.nrel.gov/electricity/data.html (accessed May 13, 2019).
[79] Carlsson J, Fortes M del MP, de Marco G, Giuntoli J, Jakubcionis M, Jäger-Waldau A, et

al. ETRI 2014 - Energy Technology Reference Indicator projections for 2010-2050. Luxembourg: European Commission; 2014. https://doi.org/10.2790/057687.
[80] Frey M, Millers U. Geothermal electricity generation in Landau. Bonn: BINE Information Service, FIZ Karlsruhe, D-76344 Eggenstein-Leopoldshafen; 2007. http://www.bine.info/fileadmin/content/Publikationen/Englische_Infos/projekt_1407_engl_Internetx.pdf.
[81] Lu S-M. A global review of enhanced geothermal system (EGS). Renew Sustain Energy Rev 2018;81:2902–21. https://doi.org/10.1016/J.RSER.2017.06.097.
[82] European Geothermal Energy Council. Developing geothermal district heating in Europe. Brussels: GeoDH report; n.d. http://www.geodh.eu.
[83] Thorsteinsson HH, Tester JW. Barriers and enablers to geothermal district heating system development in the United States. Energy Policy 2010;38:803–13. https://doi.org/10.1016/J.ENPOL.2009.10.025.
[84] [IEA] - International Energy Agency. Technology Roadmap - Geothermal Heat and Power. Paris: Renewable Energy Division, International Energy Agency, OECD/IEA; 2011. https://www.iea.org/publications/freepublications/publication/Geothermal_Roadmap.pdf.
[85] Matek B. Annual U.S. & Global Geothermal Power Production Report. Baltimore, MD: Geothermal Energy Association; 2016. http://geo-energy.org/reports.aspx.
[86] Stefánsson V. World Geothermal Assessment. Proc. World Geotherm. Congr. 2005, Antalya, Turkey: 24-29 April; 2005.
[87] Axelsson G, Stefánsson V, Björnsson G, Liu J. Sustainable Management of Geothermal Resources and Utilization for 100 – 300 Years. Proc. World Geotherm. Congr. 2005, Antalya, Turkey: 24-29 April; 2005.
[88] ITRPV Working Group. International Technology Roadmap for Photovoltaic (ITRPV) - Results 2018. Frankfurt: Tenth Edition; 2019. https://itrpv.vdma.org/download.
[89] Lazard. Lazard's levelized cost of energy analysis - version 12.0. Hamilton: 2018.
[90] Kittner N, Lill F, Kammen DM. Energy storage deployment and innovation for the clean energy transition. Nat Energy 2017;2:17125. https://doi.org/10.1038/nenergy.2017.125.
[91] Schmidt O, Hawkes A, Gambhir A, Staffell I. The future cost of electrical energy storage based on experience rates. Nat Energy 2017;6:17110. https://doi.org/10.1038/nenergy.2017.110.
[92] Shortall R, Davidsdottir B, Axelsson G. Geothermal energy for sustainable development: A review of sustainability impacts and assessment frameworks. Renew Sustain Energy Rev 2015;44:391–406. https://doi.org/10.1016/j.rser.2014.12.020.
[93] Anderson A, Rezaie B. Geothermal technology: Trends and potential role in a sustainable future. Appl Energy 2019;248:18–34. https://doi.org/10.1016/j.apenergy.2019.04.102.
[94] Bruhn D, Huenges E, Ágústsson K, Zang A, Kwiatek G, Rachez X, et al. Geothermal engineering integrating mitigation of induced seismicity in reservoirs - The European GEISER project. Trans - Geotherm Resour Counc 2011;35:1623–6.
[95] Majer E, Nelson J, Robertson-Tait A, Savy J, Wong I. Protocol for Addressing Induced Seismicity Associated with Enhanced Geothermal Systems. Washington, D.C.: U.S. Department of Energy, Energy Efficiency & Renewable Energy, Geothermal Technologies Program, DOE/EE-0662; 2012. http://www.eere.energy.gov/geothermal/.
[96] Mignan A, Karvounis D, Broccardo M, Wiemer S, Giardini D. Including seismic risk mitigation measures into the Levelized Cost Of Electricity in enhanced geothermal systems for optimal siting. Appl Energy 2019;238:831–50.

https://doi.org/10.1016/j.apenergy.2019.01.109.
[97] Moeck IS. Catalog of geothermal play types based on geologic controls. Renew Sustain Energy Rev 2014;37:867–82. https://doi.org/10.1016/j.rser.2014.05.032.